

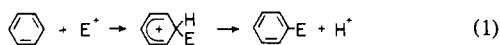
# Electrophilic Aromatic Substitution. Charge-Transfer Excited States and the Nature of the Activated Complex<sup>†</sup>

S. Fukuzumi and J. K. Kochi\*

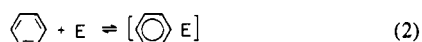
Contribution from the Department of Chemistry, Indiana University, Bloomington, Indiana 47405. Received March 18, 1981

**Abstract:** Transient charge-transfer (CT) absorption bands are observed for various benzene derivatives interacting with typical electrophiles, such as the halogens and mercuric trifluoroacetate. The second-order rate constants  $k$  for the kinetics of the disappearance of these spectral bands coincide with the rate constants for the electrophilic halogenation and mercuration of the aromatic ring. The relative reactivities ( $\log k/k_0$ ) of the arenes in electrophilic aromatic substitution are linearly related to the relative CT transition energies  $\Delta h\nu_{CT}$ , using benzene as the reference arene. This remarkable correlation thus relates the transition state for electrophilic aromatic substitution to the CT excited state  $[Ar^+E^-]^*$  of the arene-electrophile pair. Such a direct relationship requires that the solvation energies remain constant for the various aromatic cations, since the transition state is attained by an adiabatic process whereas the CT excitation involves a vertical (Franck-Condon) process. Indeed, independent measurements of the cyclic voltammetric peak potentials in acetonitrile and trifluoroacetic acid in comparison with the gas-phase ionization potentials support the constancy of the solvation term. The latter provides a ready explanation for the previously puzzling observations that the relative reactivities  $\log k/k_0$  are insensitive to solvent polarity, yet the absolute rates of electrophilic aromatic substitution are highly solvent dependent. The CT formulation for electrophilic aromatic substitution also provides a physical interpretation of the linear free energy relationship (LFER) which has been established between the  $\sigma^+$  substituent constants and the relative reactivities of arenes. The slope of the LFER correlation  $\rho$  is shown to be a measure of the mean separation in the transition state. Other LFER's found between electrophilic aromatic substitution and such parameters as the proton affinities and the  $\sigma$  and the  $\pi$  basicities of arenes are similarly interpreted. The prediction of the isomeric product distribution resulting from electron-releasing X and electron-withdrawing Y substituents is an important, natural consequence of the CT formulation. It provides unusual insight into the transition from the electron-poor arenes (Ph-Y) producing predominantly meta-substituted products to those (Ph-X) affording the para isomers.

Electrophilic aromatic substitution is one of the basic organic chemical processes, having played a key role in the development of physical organic concepts.<sup>1</sup> Extensive kinetic and mechanistic studies have led to the general consensus that a  $\sigma$  complex or benzenium ion occurs along the reaction coordinate leading to aromatic substitution by various electrophiles  $E^+$ , as in eq 1.<sup>1,2</sup>



Indeed, the independent existence of such reactive intermediates as distinct chemical entities has been demonstrated with numerous electrophiles, notably in a series of elegant studies by Olah and co-workers.<sup>3</sup> However, there is surprisingly little fundamental information as to the quantitative description of the activation barrier leading to aromatic substitution by various electrophiles. A number of discussions have centered around qualitative descriptions of transition-state structures, particularly as to whether they resemble  $\sigma$  complexes or  $\pi$  complexes.<sup>4</sup> (Although there are different definitions of the  $\pi$ -complex extant, the electron donor-acceptor complexes of arenes and electrophiles, i.e., eq 2,



can in practice serve as a general model.<sup>5</sup>) A distinction between the  $\sigma$  complex and the  $\pi$  complex as the appropriate transition-state model has been put forth by using the relative reactivity of benzene and toluene as an index.<sup>6</sup>

Comprehensive mechanistic analyses have been carried out for numerous electrophilic aromatic substitutions based on the linear free energy relationship which has been observed between the Brown  $\sigma^+$  constants and the relative rates (i.e.,  $\log k/k_0$ , using benzene as the reference).<sup>7</sup> The slopes of the correlation, i.e., the  $\rho$  values, are especially noteworthy. For example, the  $\rho$  values are singularly insensitive to the solvent polarity, despite large solvent effects on the absolute rates of electrophilic substitution.<sup>8</sup> Various electrophiles have characteristic  $\rho$  values, which vary from -4 for mercuration with  $\text{Hg}(\text{OAc})_2$  to -12 for bromination with  $\text{Br}_2$  in acetic acid.<sup>18</sup> Since the  $\rho$  value measures the arene sen-

sitivity to electrophilic substitution, it has been viewed as a reflection of electrophile reactivity—the more reactive electrophiles inducing lower substrate selectivities.<sup>9</sup> However appealing the

(1) (a) Taylor, R. In "Comprehensive Chemical Kinetics"; Bamford, C. H.; Tipper, C. F. H., Ed.; Elsevier: London, 1972; Vol. 13. (b) de la Mare, P. B. D. "Electrophilic Halogenation"; Cambridge University Press: London, 1976. (c) Olah, G. A. *Acc. Chem. Res.* 1971, 4, 240. (d) de la Mare, P. B. D. *Acc. Chem. Res.* 1974, 7, 361. (e) Norman, R. O. C.; Taylor, R. "Electrophilic Substitution in Benzenoid Compounds"; American Elsevier: New York, 1965. (f) Banthorpe, D. V. *Chem. Rev.* 1970, 70, 295. (g) Stock, L. M.; Brown, H. C. *Adv. Phys. Org. Chem.* 1963, 1, 35. (h) Stock, L. M. "Aromatic Substitution Reactions"; Prentice-Hall: Englewood Cliffs, NJ, 1968. (i) Bloodworth, A. J. In "The Chemistry of Mercury"; McAuliffe, C. A., Ed.; MacMillan: Toronto, 1977; p 152. (j) Smith, B. V. In "Organic Reaction Mechanism"; Butler, A. R.; Perkins, M. J., Ed.; Wiley Interscience: New York, 1977; Chapter 7. (k) Todres, Z. V. *Russ. Chem. Rev. (Engl. Transl.)* 1978, 47, 148. (l) Stock, L. M. *Prog. Phys. Org. Chem.* 1976, 12, 21. (m) Skrabal, P. R. P.; Zollinger, H. *Angew. Chem., Int. Ed. Engl.* 1972, 11, 874.

(2) The benzenium is defined as a trivalent cyclohexadienyl cation (Olah, G. A. *J. Am. Chem. Soc.* 1972, 94, 808) and is also referred to as a Wheland intermediate in electrophilic aromatic substitution (Wheland, G. W. *Ibid.* 1942, 64, 900).

(3) (a) Olah, G. A. "Carbocations and Electrophilic Reactions"; Verlag Chemie and Wiley: New York, 1974, p 38 and references cited therein. (b) Brouwer, D. M.; Mackor, E. L.; MacLean, C. *Carbonium Ions* 1970, 2 (Chapter 20), 837. (c) Olah, G. A.; Mo, Y. K. *Ibid.* 1976, 5 (Chapter 36), 2202. (d) Olah, G. A.; Yu, S. H.; Parker, D. G. *J. Org. Chem.* 1976, 41, 1983.

(4) See discussions in ref 1a, p 198; 1c; 1e, p. 31; 1f; 1k; 1l and 1m.

(5) For the confusion regarding the definition of  $\pi$  complexes see ref 1f. The  $\pi$  complex as a reactive intermediate is postulated to have a three-centered bond by Dewar.<sup>14c</sup> Such a nonclassical bridged carbonium ion is classified as a benzenonium ion in ref 2. This  $\pi$  complex is distinguished from the experimentally verifiable molecular complex such as the electron donor-acceptor complex. The EDA complex has been designated as an outer complex, thus, to differentiate it from the  $\pi$  complex or inner complex. However, since no direct experimental evidence exists for such postulated  $\pi$  complexes (Brown, H. C. "The Nonclassical Ion Problem"; Plenum Press: New York, 1977; p 47), the stabilities of the EDA complex have been used to support  $\pi$  complexes as reactive intermediates, especially in the comparison of the relative rates.

(6) The reactivity of toluene relative to benzene was believed to be greater for a  $\sigma$ -like (benzenonium ion) transition state compared to a  $\pi$ -like (benzenonium ion) one. Owing to their resemblance to the starting arene, substituents were considered to have little effect on  $\pi$ -like transition states of low activation energies.

(7) (a) See ref 1g. (b) For recent reviews see: Pross, A. *Adv. Phys. Org. Chem.* 1977, 14, 69. Chapman, N. B.; Shorter, J. "Correlation Analysis in Chemistry"; Plenum Press: New York, 1978.

<sup>†</sup> Dedicated to George S. Hammond on the joyous occasion of his 60th birthday.

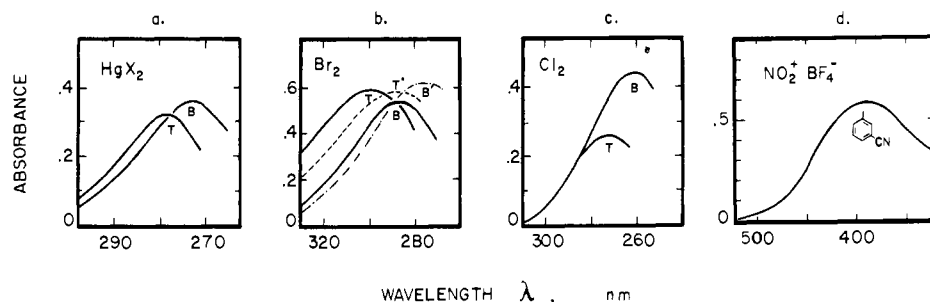


**Figure 1.** Charge-transfer absorption spectra of benzene (B) and toluene (T) with electrophiles: (a) mercuric trifluoroacetate in methylene chloride, (b) bromine in carbon tetrachloride (solid line) and in trifluoroacetic acid (broken lines), (c) chlorine in carbon tetrachloride, (d) CT spectrum of *m*-tolunitrile and nitronium fluoroborate in acetonitrile.

notion of the variable transition state may be, no general rule for reactivity-selectivity exists for electrophilic aromatic substitutions.<sup>10</sup> Such large unaccountable variations in the arene selectivities with various electrophiles have thus spawned alternative formulations, such as those based on the  $\pi$  complex, the contribution of which is electrophile dependent.<sup>5</sup>

One qualitative criterion to differentiate between  $\sigma$  and  $\pi$  complexes as transition-state models rests on the comparison of the reactivity of arenes with their  $\sigma$  and  $\pi$  basicities,<sup>1c</sup> which are experimentally available from the acids HF/BF<sub>3</sub><sup>11</sup> and HCl,<sup>12</sup> respectively. Unfortunately such parameters do not include any provision for changes in the nature of the  $\sigma$  or  $\pi$  complex arising from the use of different electrophiles. Moreover, there is no assurance that the transition states would even resemble the  $\sigma$  or  $\pi$  complex from which their basicities are derived.<sup>13</sup> Here we encounter a more serious conceptual dilemma: the stabilities of complexes, even if they could be successfully measured for various electrophiles, must automatically show significant deviations from activated complexes lying at energy *maxima*. At this juncture the mechanistic situation summarized above is at an impasse.

Theoretical approaches to electrophilic aromatic substitution have generally been based on the interaction of the highest occupied molecular orbital (HOMO) of the arene and the lowest unoccupied orbitals (LUMO) of the electrophile, using either the perturbation theory or other methods.<sup>14</sup> Although they have provided guides to the trends in arene reactivity, no quantitative treatment has yet resulted, especially with regard to steric effects and solvent effects.<sup>15</sup> We have approached this mechanistic problem from an entirely different approach which stems from our studies of charge-transfer (CT) interactions.<sup>16</sup> In this formulation, the CT excited state of the arene and electrophile is related directly to the activation barrier to electrophilic aromatic substitution. We wish to show how the charge-transfer formulation

provides physical insight into the transition state for electrophilic substitution, particularly with regard to the significance of the  $\rho$  values and the solvent effects. The CT formulation also yields a unique insight into the origin of the isomeric product distribution.

## Results

For the mechanistic study of electrophilic aromatic substitution, we chose the halogens (Cl<sub>2</sub>, Br<sub>2</sub>) and the mercuric complex [Hg(O<sub>2</sub>CCF<sub>3</sub>)<sub>2</sub>] as representatives of structurally diverse electrophiles. In each case, the experimental problem initially centered on the measurement of the charge-transfer (CT) absorption spectrum of the electron donor-acceptor (EDA) complex of those electrophiles with various aromatic compounds. The observation of these transient CT spectra was carried out in competition with the substitution reactions leading to electrophilic halogenation or mercuration of the aromatic ring.

**I. Charge-Transfer Absorption Spectra of Electrophiles with Aromatic Compounds.** A new absorption band appears immediately upon mixing mercuric trifluoroacetate and benzene or toluene in methylene chloride solutions at 25 °C. Since the absorption maximum occurs in the ultraviolet region, the *difference spectrum* in Figure 1a was measured under carefully calibrated conditions, as described in the Experimental Section. Similar broad absorption bands observed with benzene and bromine (Figure 1b) or with chlorine (Figure 1c) are all characteristic of intermolecular electron donor-acceptor or EDA complexes,<sup>17</sup> e.g. eq 3, where E = Hg(O<sub>2</sub>CCF<sub>3</sub>)<sub>2</sub>, Br<sub>2</sub>, and Cl<sub>2</sub>. The 1:1 stoichiometry of these EDA complexes has been confirmed by the linear dependence of the CT absorbance  $\mathcal{A}$  on the concentration of each component according to the Benesi-Hildebrand formulation,<sup>18</sup> i.e.

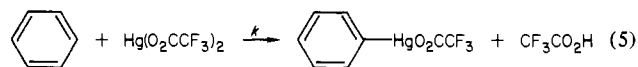


where  $K_{\text{DA}}$  and  $\epsilon$  are the formation constant and the extinction coefficient of the complex, respectively, and [E] is the concentration of the electrophile Hg(O<sub>2</sub>CCF<sub>3</sub>)<sub>2</sub>, Br<sub>2</sub>, or Cl<sub>2</sub>.<sup>19</sup> The charge-transfer spectrum of *m*-tolunitrile and nitronium fluoroborate is included in Figure 1d for comparison, since benzene and toluene are too reactive.<sup>1-3</sup>

$$\mathcal{A} = \epsilon K_{\text{DA}} [\text{C}_6\text{H}_6] [\text{E}] \quad (4)$$

where  $K_{\text{DA}}$  and  $\epsilon$  are the formation constant and the extinction coefficient of the complex, respectively, and [E] is the concentration of the electrophile Hg(O<sub>2</sub>CCF<sub>3</sub>)<sub>2</sub>, Br<sub>2</sub>, or Cl<sub>2</sub>.<sup>19</sup> The charge-transfer spectrum of *m*-tolunitrile and nitronium fluoroborate is included in Figure 1d for comparison, since benzene and toluene are too reactive.<sup>1-3</sup>

**II. Rates of Electrophilic Aromatic Substitution. A. Mercuration of Arenes by Mercuric Trifluoroacetate.** The decay of the transient CT absorption band arising from the interaction of benzene and mercuric trifluoroacetate is associated with the mercuration process, the products and stoichiometry of which have been well-established as<sup>20</sup>



(17) (a) Mulliken, R. S.; Person, W. B. "Molecular Complexes"; Wiley-Interscience: New York, 1969. (b) Foster, R. "Organic Charge Transfer Complexes"; Academic Press: New York, 1969.

(18) Benesi, H. A.; Hildebrand, J. H. *J. Am. Chem. Soc.* **1949**, *71*, 2703.

(19) The nature of the charge-transfer spectra arising from the interaction of various electrophiles with a series of substituted benzenes has been elaborated in a separate study. See ref 16.

(8) This is one factor which allows the Brown  $\sigma^+$  constant to be so comprehensive. By the same token, it fails to provide information about the larger solvent effects on the absolute rates. See: Johnson, C. D. *Chem. Rev.* **1975**, *75*, 755.

(9) E.g.: Altschuler, L.; Berliner, E. *J. Am. Chem. Soc.* **1966**, *88*, 5837.

(10) For example, the more reactive electrophile (Br<sub>2</sub>) yields a larger  $\rho$  value (-12.1) than Hg(OAc)<sub>2</sub> ( $\rho = -4.0$ ).

(11) (a) Mackor, E. L.; Hofstra, A.; van der Waals, J. H. *Trans. Faraday Soc.* **1958**, *54*, 66, 187. (b) Andrews, L. J. *Chem. Rev.* **1954**, *54*, 713.

(12) Brown, H. C.; Brady, J. D. *J. Am. Chem. Soc.* **1952**, *74*, 3570.

(13) Thus, there is no quantitative criterion as to how linear the plots should be, or what the slopes should be. Sometimes, the plot of the relative reactivities against neither the  $\sigma$  nor the  $\pi$  basicities affords good linear correlations (see ref 1j).

(14) (a) Fukui, K.; Yonezawa, T.; Nagata, C.; Shingu, H. *J. Chem. Phys.* **1954**, *22*, 1433. (b) Brown, R. D. *J. Chem. Soc.* **1959**, 2232. (c) Nagakura, S.; Tanaka, J. *Bull. Chem. Soc. Jpn.* **1959**, *32*, 734. (d) Nagakura, S. *Tetrahedron, Suppl.* **2** **1963**, *19*, 361. (e) Dewar, M. J. S. "The Molecular Orbital Theory of Organic Chemistry"; McGraw-Hill: New York, 1969. (f) Epiotis, N. D. *J. Am. Chem. Soc.* **1973**, *95*, 3188. (g) Greenwood, H. H.; McWeeny, R. *Adv. Phys. Org. Chem.* **1966**, *4*, 73. (h) Epiotis, N. D.; Shaik, S. *J. Am. Chem. Soc.* **1978**, *100*, 29. (i) Takabe, T.; Takenaka, K.; Yamaguchi, K.; Fueno, T. *Chem. Phys. Lett.* **1976**, *44*, 65.

(15) For example, the large solvent effect on the absolute rates of the chlorination of benzene follows the order ClCH<sub>2</sub>CH<sub>2</sub>Cl  $\ll$  Ac<sub>2</sub>O  $\approx$  AcOH  $\approx$  CH<sub>3</sub>CN  $<$  CH<sub>3</sub>NO<sub>2</sub>  $\ll$  CF<sub>3</sub>CO<sub>2</sub>H. (Andrews, L. J.; Keefer, R. M. *J. Am. Chem. Soc.* **1959**, *81*, 1063; **1957**, *79*, 5169.)

(16) Fukuzumi, S.; Kochi, J. K. *J. Org. Chem.*, **1981**, *46*, 4116.

Table I. Kinetics of Mercuration of Benzene Derivatives in Methylene Chloride and in Trifluoroacetic Acid at 25 °C

no.	aromatic compd	$h\nu_{CT},^a$ eV	methylene chloride		trifluoroacetic acid	
			$k,^b$ M <sup>-1</sup> s <sup>-1</sup>	$\log(k/k_0)^c$	$k,^d$ M <sup>-1</sup> s <sup>-1</sup>	$\log(k/k_0)^c$
1	C <sub>6</sub> H <sub>6</sub>	4.54	1.0 × 10 <sup>-4</sup>	0	2.9 × 10 <sup>-2</sup>	0
2	<i>o</i> -Cl <sub>2</sub> C <sub>6</sub> H <sub>4</sub>		1.5 × 10 <sup>-6</sup>	-1.82		
3	ClC <sub>6</sub> H <sub>5</sub>	4.64	2.1 × 10 <sup>-6</sup>	-1.68	8.3 × 10 <sup>-4</sup>	-1.54
4	BrC <sub>6</sub> H <sub>5</sub>	4.59	3.2 × 10 <sup>-5</sup>	-0.50	1.1 × 10 <sup>-3 e</sup>	-1.42
5	MeC <sub>6</sub> H <sub>5</sub>	4.46	9.9 × 10 <sup>-4</sup>	1.00	5.1 × 10 <sup>-1</sup>	1.25
6	EtC <sub>6</sub> H <sub>5</sub>	4.46	1.0 × 10 <sup>-3</sup>	1.61	2.4 × 10 <sup>-1 e</sup>	0.92
7	<i>n</i> -PrC <sub>6</sub> H <sub>5</sub>	4.44	1.6 × 10 <sup>-3</sup>	1.63		
8	<i>n</i> -BuC <sub>6</sub> H <sub>5</sub>	4.46	1.3 × 10 <sup>-3</sup>	1.12		
9	<i>i</i> -PrC <sub>6</sub> H <sub>5</sub>	4.44	1.2 × 10 <sup>-3</sup>	1.40	2.1 × 10 <sup>-1 e</sup>	0.86
10	<i>t</i> -BuC <sub>6</sub> H <sub>5</sub>	4.46	1.3 × 10 <sup>-3</sup>	1.12	1.7 × 10 <sup>-1 e</sup>	0.77
11	MeOC <sub>6</sub> H <sub>5</sub>		3.7 × 10 <sup>-1</sup>	3.30		
12	<i>o</i> -Me <sub>2</sub> C <sub>6</sub> H <sub>4</sub>	4.41	4.8 × 10 <sup>-3</sup>	1.68	2.8	1.98
13	<i>m</i> -Me <sub>2</sub> C <sub>6</sub> H <sub>4</sub>	4.41	4.3 × 10 <sup>-2</sup>	2.63	1.0 × 10 <sup>f</sup>	2.54
14	<i>p</i> -Me <sub>2</sub> C <sub>6</sub> H <sub>4</sub>	4.43	3.9 × 10 <sup>-3</sup>	1.60	1.2 <sup>f</sup>	1.62
15	<i>p</i> - <i>i</i> -PrC <sub>6</sub> H <sub>4</sub> Me	4.43	3.2 × 10 <sup>-3</sup>	1.51		
16	<i>o</i> -ClC <sub>6</sub> H <sub>4</sub> Me	4.56	8.5 × 10 <sup>-5</sup>	-0.07		
17	<i>m</i> -ClC <sub>6</sub> H <sub>4</sub> Me	4.54	7.2 × 10 <sup>-5</sup>	-0.14		
18	<i>p</i> -ClC <sub>6</sub> H <sub>4</sub> Me	4.51	1.9 × 10 <sup>-5</sup>	-0.72		
19	<i>m</i> -BrC <sub>6</sub> H <sub>4</sub> Me	4.54	6.4 × 10 <sup>-5</sup>	-0.20		
20	<i>p</i> -BrC <sub>6</sub> H <sub>4</sub> Me	4.51	1.3 × 10 <sup>-5</sup>	-0.89		
21	1,3,5-Me <sub>3</sub> C <sub>6</sub> H <sub>3</sub>	4.30	4.6 × 10 <sup>-1</sup>	3.66	1.7 × 10 <sup>3 f</sup>	4.77
22	1,2,3,4-Me <sub>4</sub> C <sub>6</sub> H <sub>2</sub>				6.7 × 10 <sup>3 f</sup>	5.36
23	1,2,4,5-Me <sub>4</sub> C <sub>6</sub> H <sub>2</sub>				3.9 × 10 <sup>3 f</sup>	5.13
24	Me <sub>6</sub> C <sub>6</sub>	3.84	<i>g</i>			
25	Et <sub>6</sub> C <sub>6</sub>	3.94	<i>g</i>			

<sup>a</sup> In methylene chloride.<sup>16</sup> <sup>b</sup> Experimental error < ±20%. <sup>c</sup> Relative rate constants using benzene as the reference. <sup>d</sup> From ref 23. <sup>e</sup> From ref 20a. <sup>f</sup> No reaction ( $k \ll 10^{-7}$  M<sup>-1</sup> s<sup>-1</sup>).

Thus the progress of mercuration could be monitored spectroscopically by directly following the decrease in the CT absorbance in Figure 1b. The same kinetic results were obtained by following the disappearance of mercuric trifluoroacetate. The latter method involved the quantitative conversion of mercuric trifluoroacetate to triiodomercurate(II), by periodic sampling of the reaction mixture, followed by rapid quenching with excess potassium iodide. The concentration of triiodomercurate(II) was determined spectrophotometrically at 301.5 nm, using the calibrated equation developed by Abraham and Johnston.<sup>21,22</sup> Generally, the CT absorbance change was conveniently applied to electron-rich arenes undergoing rapid mercuration, whereas the iodide quench was suitable for following the progress of the relatively slow reactions.

The rate of disappearance of mercuric trifluoroacetate can be expressed by second-order kinetics as

$$\frac{-d[\text{Hg}(\text{O}_2\text{CCF}_3)_2]}{dt} = k[\text{C}_6\text{H}_6][\text{Hg}(\text{O}_2\text{CCF}_3)_2] \quad (6)$$

which was confirmed both under actual second-order conditions and under pseudo-first-order conditions in the presence of excess arene. The linear plots in Figure 2 (left) were obtained with equimolar amounts of mercuric trifluoroacetate and various arenes, and those in Figure 2 (right) were obtained with the arene in excess. The monitoring of the CT and the HgI<sub>3</sub><sup>-</sup> absorbances yielded essentially the same kinetic results, as described in detail in the Experimental Section.

The second-order rate constants  $k$  for the mercuration of a series of substituted benzenes are listed in Table I, together with the CT absorption maxima in methylene chloride as the common solvent. It is noteworthy in Table I that the increase in the rate constant for mercuration in proceeding from chlorobenzene ( $k = 2.1 \times 10^{-6}$  M<sup>-1</sup> s<sup>-1</sup>) to mesitylene ( $0.46$  M<sup>-1</sup> s<sup>-1</sup>) occurs in parallel with the corresponding decrease in the CT transition energies of chlorobenzene ( $h\nu_{CT} = 4.64$  eV) relative to mesitylene (4.30 eV). The highly encumbered hexa-substituted benzenes such as hexamethylbenzene and hexaethylbenzene, however, are the excep-

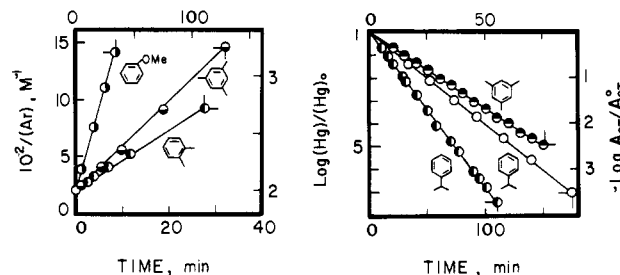


Figure 2. Kinetics of mercuration: (a) left, second-order plots for the disappearance of  $5.0 \times 10^{-3}$  M arene and  $\text{Hg}(\text{O}_2\text{CCF}_3)_2$  in  $\text{CH}_2\text{Cl}_2$  at 25 °C; (b) Right, pseudo-first-order plots for the disappearance of  $\text{Hg}(\text{O}_2\text{CCF}_3)_2$  and the decay of the CT absorbance (●, CT at 355 nm,  $7.12 \times 10^{-2}$  M mesitylene and  $1.0 \times 10^{-2}$  M  $\text{Hg}(\text{O}_2\text{CCF}_3)_2$  time scale at the top of the figure in units of seconds; ○, CT at 300 nm,  $7.12 \times 10^{-2}$  M cumene and  $1.0 \times 10^{-2}$  M  $\text{Hg}(\text{O}_2\text{CCF}_3)_2$ ; ●, Hg,  $5.0 \times 10^{-2}$  M cumene and  $5.0 \times 10^{-3}$  M  $\text{Hg}(\text{O}_2\text{CCF}_3)_2$ ).

tions, since they are unreactive to mercuric trifluoroacetate despite the substantially lower values of their ionization potentials of 3.84 and 3.94 eV, respectively.

The solvent effects in mercuration are manifested in the second-order rate constants in trifluoroacetic acid, some of which were reported earlier.<sup>20,23</sup> Although the absolute values of the rate constants in trifluoroacetic acid are substantially larger than those in methylene chloride (compare Table I, columns 4 and 6), the relative rate constants  $\log k/k_0$  using benzene as a reference are similar in both solvents (compare columns 5 and 7).

**B. Bromination of Aromatic Compounds.** The bromination of aromatic compounds occurs readily in trifluoroacetic acid, and it follows second-order kinetics, e.g.<sup>24</sup>

$$-d[\text{Br}_2]/dt = k[\text{C}_6\text{H}_6][\text{Br}_2] \quad (7)$$

(23) Fung, C. W.; Khorramdel-Vahed, M.; Ranson, R. J.; Roberts, R. M. *J. Chem. Soc., Perkin Trans. 2* 1980, 267.

(20) (a) Olah, G. A.; Hashimoto, I.; Lin, H. C. *Proc. Natl. Acad. Sci. U.S.A.* 1977, 74, 4121. (b) Brown, H. C.; Wirkkala, R. A. *J. Am. Chem. Soc.* 1966, 88, 1453, 1456.

(21) Abraham, M. H.; Johnston, G. F. *J. Chem. Soc. A* 1970, 188.

(22) Fukuzumi, S.; Kochi, J. K. *J. Am. Chem. Soc.* 1980, 102, 7290.

(24) Brominations of aromatic compounds have been extensively studied in acetic acid.<sup>25</sup> However, the rates in this medium follow complex kinetics, being a combination of second-order (first order in  $\text{Br}_2$ ) and third-order terms (second order in  $\text{Br}_2$ ).<sup>25c,d</sup> Brown and Wirkkala<sup>26</sup> showed the utility of trifluoroacetic acid as a reaction medium in which bromination proceeds much more readily than in acetic acid and follows simple second-order kinetics.

Table II. Second-Order Rate Constants and Relative Rates for the Bromination and Chlorination of Benzene Derivatives in Trifluoroacetic Acid and in Acetic Acid at 25 °C

aromatic compd <sup>a</sup> no.	bromination				chlorination	
	$h\nu_{CT},^b$ eV	trifluoroacetic acid		acetic acid	acetic acid	
		$k, M^{-1} s^{-1}$	$\log(k/k_0)$	$\log(k/k_0)^d$	$h\nu_{CT},^g$ eV	$\log(k/k_0)^h$
1	4.32 (4.49)	$7.7 \times 10^{-7}^c$	0	0	4.75	0 <sup>i</sup>
3	4.43 (4.57)	$1.0 \times 10^{-7}$	-0.89			-1.00
4	4.35 (4.54)	$9.0 \times 10^{-8}$	-0.93			-1.14
5	4.15 (4.30)	$2.2 \times 10^{-3}^c$	3.46	2.78	4.56	2.56 <sup>j</sup>
6	4.15 (4.30)	$3.1 \times 10^{-3}^c$	3.60	2.66 <sup>e</sup>	4.57	2.46
7	4.15 (4.29)	$3.6 \times 10^{-3}^c$	3.67			
8	4.15 (4.29)	$4.2 \times 10^{-3}$	3.74		4.56	
9	4.13 (4.30)	$2.7 \times 10^{-3}^c$	3.54	2.41 <sup>e</sup>	4.56	2.26
10	4.15 (4.30)	$2.4 \times 10^{-3}^c$	3.49		4.61	1.94
11	3.73			9.26 <sup>e</sup>	4.13	
12	4.00 (4.17)	$4.0 \times 10^{-2}^c$	4.72	3.73	4.46	3.59 <sup>j</sup>
13	3.97	3.7	6.68	5.74	4.43	5.44 <sup>j</sup>
14	4.13 (4.27)	$1.7 \times 10^{-2}^c$	4.34	3.40	4.48	3.35 <sup>j</sup>
15	4.09 (4.26)	$2.3 \times 10^{-2}$	4.48		4.49	
16	4.23 (4.41)	$6.6 \times 10^{-6}$	0.93			
17	4.27 (4.40)	$1.6 \times 10^{-4}$	2.32			
18	4.35 (>4.43)	$1.2 \times 10^{-6}$	0.19			-0.30
19	4.23 (4.38)	$1.3 \times 10^{-4}$	2.23			
20	4.25 (4.43)	$2.0 \times 10^{-6}$	0.41			-0.31
21	3.79	$1.6 \times 10^2$	8.32	8.28 <sup>f</sup>	4.27	8.04 <sup>k</sup>
22	3.78					
23	3.77				4.32	6.43 <sup>l</sup>
24	3.36	$1.6 \times 10^{-1}$	5.32		3.87	
25	3.41					

<sup>a</sup> Identified in Table I. <sup>b</sup> CT transition energy of the Br<sub>2</sub> complexes with arenes in CCl<sub>4</sub>; values in parentheses in CF<sub>3</sub>CO<sub>2</sub>H.<sup>16</sup> <sup>c</sup> Similar values are reported in ref 20b. <sup>d</sup> Taken from ref 25a. <sup>e</sup> From ref 25b. <sup>f</sup> Absolute rate constants  $k_1$  (second order) =  $4.5 \times 10^{-4} M^{-1} s^{-1}$ ,  $k_2$  (third order) =  $2.6 M^{-1} s^{-1}$  from ref 25c. <sup>g</sup> CT transition energy of the Cl<sub>2</sub> complexes with arenes in CCl<sub>4</sub> from ref 16. <sup>h</sup> From ref 30a. <sup>i</sup> The absolute rate constant:  $1.54 \times 10^{-6} M^{-1} s^{-1}$ , from ref 30b. <sup>j</sup> The average value was taken from ref 30b-d. <sup>k</sup> From ref 30c and e. <sup>l</sup> From ref 30d.

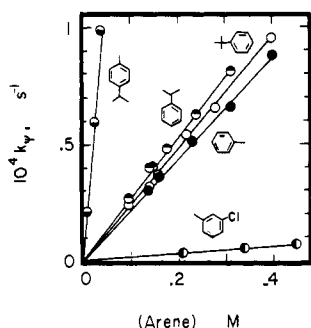


Figure 3. Kinetics of the bromination of substituted benzenes in trifluoroacetic acid at 25 °C under pseudo-first-order conditions with  $[Br_2]_0 = 5.43 \times 10^{-3} M$ : ○, *p*-cumene; ●, cumene; ○, *tert*-butylbenzene; ●, toluene; ●, *m*-chlorotoluene.

In order to compare bromination directly with mercuration in Table I, we measured the second-order rate constants for the bromination of the same series of benzene derivatives under equivalent reaction conditions.

The rates of bromination were followed by monitoring the decay of the transient CT bands<sup>27</sup> listed in Table II. The rates of

(25) (a) Brown, H. C.; Stock, L. M. *J. Am. Chem. Soc.* **1957**, *79*, 1421. (b) Stock, L. M.; Brown, H. C. *Ibid.* **1959**, *82*, 1942. (c) Keefer, R. M.; Andrews, L. J. *Ibid.* **1956**, *78*, 255. (d) Keefer, R. M.; Andrews, L. J. *Ibid.* **1977**, *99*, 5693. (e) Robertson, P. W. *J. Chem. Soc.* **1954**, 1276. (f) Robertson, P. W.; de la Mare, P. B. D.; Johnston, W. T. G. *Ibid.* **1943**, 276. (g) Seshadri, K. V.; Ganesan, R. Z. *Phys. Chem. (Wiesbaden)* **1968**, *62*, 29. (26) Brown, H. C.; Wirkkala, R. A. *J. Am. Chem. Soc.* **1966**, *88*, 1447.

(27) (a) The kinetics of bromination have been followed titrimetrically by using thiosulfate.<sup>26</sup> We used the spectroscopic method in order to examine the involvement of arene-bromine EDA complex.<sup>28</sup> The same results are obtained from both kinetic methods. (b) The shape of the CT band in carbon tetrachloride indicated by the solid line in Figure 1b is quite similar to that in trifluoroacetic acid (broken line). The solvent-induced blue shift in  $\lambda_{max}$  is a constant, irrespective of the arene,<sup>16</sup> and it may be caused by a specific solvation of CF<sub>3</sub>CO<sub>2</sub>H to the benzene ring (see, e.g.: Dannenberg, J. J. *Angew. Chem., Int. Ed. Engl.* **1975**, *14*, 641). (c) The decay of the CT band was followed at the wavelengths where only the CT band is observed, with minimal overlap with the absorbance from the reactants (see Experimental Section).

bromination in trifluoroacetic acid were also followed by monitoring the disappearance of the bromine absorbance [ $\lambda_{max}$  411 nm ( $\epsilon_{max}$  138 M<sup>-1</sup> cm<sup>-1</sup>)].<sup>29</sup> The pseudo-first-order rate constants showed a linear dependence on the arene present in excess, as illustrated in Figure 3. The second-order rate constants obtained in this manner, and listed in Table II, coincided with those obtained from the disappearance of the CT absorption band. (See the Experimental Section for details.) The relative reactivities ( $\log k/k_0$ ) in acetic acid for various arenes using benzene as the reference are also included in Table II (column 6) together with the data taken from the extant literature.<sup>25</sup> The relative reactivities of various arenes in trifluoroacetic acid are more or less parallel to those in acetic acid, as shown by a comparison of the data in columns 5 and 6 in Table II.

**C. Chlorination of Aromatic Compounds.** The chlorination of aromatic compounds is generally known to follow straight second-order kinetics, even in acetic acid media.<sup>15,30</sup> For most of the arenes examined in this study, the rates of chlorination in trifluoroacetic acid were too fast to follow by conventional techniques. The relative reactivities of substituted benzenes toward chlorination in acetic acid are tabulated in the last column of Table II. The CT transition energies of the corresponding chlorine-arene EDA complexes (compare Figure 1c) are also listed in the table. It is noteworthy that the relative reactivities of various arenes in chlorination generally parallel those in bromination (see Table II), but both electrophilic processes differ substantially from mercuration (compare Table I).

### III. Cyclic Voltammetry of Benzene Derivatives. The cyclic

(28) The crystal structure of benzene-halogen complexes is known to have C<sub>6h</sub> symmetry. See the review by: Hassel, O.; Rømming, C. *Q. Rev., Chem. Soc.* **1962**, *16*, 1.

(29) Buckles, R. E.; Mills, J. F. *J. Am. Chem. Soc.* **1953**, *75*, 552.

(30) (a) Stock, L. M.; Baker, F. W. *J. Am. Chem. Soc.* **1962**, *84*, 1661. (b) Brown, H. C.; Stock, L. M. *Ibid.* **1957**, *79*, 5175. (c) de la Mare, P. B. D.; Robertson, P. W. *J. Chem. Soc.* **1943**, 279. (d) Keefer, R. M.; Andrews, L. J. *J. Am. Chem. Soc.* **1957**, *79*, 4348. (e) Baciocchi, E.; Illuminati, G. *Ibid.* **1964**, *86*, 2677; *Chem. Ind. (London)* **1958**, 917. (f) Novrocik, J.; Poskocil, J.; Cepciansky, I. *Collect. Czech., Chem. Commun.* **1978**, *43*, 1488. (g) Baciocchi, E.; Mandolini, L. *J. Chem. Soc. B* **1967**, 1361.

Table III. Cyclic Voltammetric Data for Benzene Derivatives in Acetonitrile and in Trifluoroacetic Acid<sup>a</sup>

no.	aromatic compd	$I_D^b$ eV	acetonitrile <sup>e</sup>		trifluoroacetic acid <sup>e</sup>	
			$E_p^f$ V	$E_p - E_{p/2}$ V	$E_p^f$ V	$E_p - E_{p/2}$ V
1	C <sub>6</sub> H <sub>6</sub>	9.23	2.83	0.24	2.62	0.30
2	<i>o</i> -Cl <sub>2</sub> C <sub>6</sub> H <sub>4</sub>	9.12 <sup>c</sup>	2.81	0.23	2.68	0.38
3	ClC <sub>6</sub> H <sub>5</sub>	9.08	2.76	0.22	2.58	0.36
4	BrC <sub>6</sub> H <sub>5</sub>	9.05	2.65	0.18	2.50	0.35
5	MeC <sub>6</sub> H <sub>5</sub>	8.82	2.39	0.17	2.29	0.41
6	EtC <sub>6</sub> H <sub>5</sub>	8.76	2.39	0.15	2.25	0.35
7	<i>n</i> -PrC <sub>6</sub> H <sub>5</sub>	8.72	2.38	0.14	2.28	0.36
8	<i>n</i> -BuC <sub>6</sub> H <sub>5</sub>	8.69	2.36	0.14	2.28	0.42
9	<i>t</i> -PrC <sub>6</sub> H <sub>5</sub>	8.69	2.46	0.18	2.19	0.34
10	<i>i</i> -BuC <sub>6</sub> H <sub>5</sub>	8.68	2.51	0.19	2.29	0.30
11	MeOC <sub>6</sub> H <sub>5</sub>	8.39	1.96	0.15	1.89	0.28
12	<i>o</i> -Me <sub>2</sub> C <sub>6</sub> H <sub>4</sub>	8.56	2.23	0.14	2.11	0.36
13	<i>m</i> -Me <sub>2</sub> C <sub>6</sub> H <sub>4</sub>	8.56	2.27	0.14	1.95	0.30
14	<i>p</i> -Me <sub>2</sub> C <sub>6</sub> H <sub>4</sub>	8.44	2.15	0.14	1.95	0.31
15	<i>p</i> - <i>i</i> -PrC <sub>6</sub> H <sub>4</sub> Me		2.21	0.16	2.11	0.32
16	<i>o</i> -ClC <sub>6</sub> H <sub>4</sub> Me	8.83	2.48	0.14	2.37	0.27
17	<i>m</i> -ClC <sub>6</sub> H <sub>4</sub> Me	8.83	2.48	0.15	2.25	0.25
18	<i>p</i> -ClC <sub>6</sub> H <sub>4</sub> Me	8.69	2.36	0.14	2.18	0.21
19	<i>m</i> -BrC <sub>6</sub> H <sub>4</sub> Me	8.81	2.46	0.14	2.22	0.29
20	<i>p</i> -BrC <sub>6</sub> H <sub>4</sub> Me	8.67	2.32	0.14	2.09	0.28
21	1,3,5-Me <sub>3</sub> C <sub>6</sub> H <sub>3</sub>	8.40	2.10	0.13	1.78	0.27
22	1,2,3,4-Me <sub>4</sub> C <sub>6</sub> H <sub>2</sub>		1.89	0.10	1.68	0.23
23	1,2,4,5-Me <sub>4</sub> C <sub>6</sub> H <sub>2</sub>	8.05	1.90	0.11	1.55	0.21
24	Me <sub>6</sub> C <sub>6</sub>	7.85	1.69	0.10	1.26	0.14
25	Et <sub>6</sub> C <sub>6</sub>		1.83	0.10	1.39	0.11
26	<i>m</i> -MeOC <sub>6</sub> H <sub>4</sub> Me	8.28 <sup>d</sup>	1.80	0.11	1.79	0.34
27	<i>p</i> -MeOC <sub>6</sub> H <sub>4</sub> Me	8.18 <sup>d</sup>	1.71	0.07	1.71	0.29
28	<i>m</i> -(MeO) <sub>2</sub> C <sub>6</sub> H <sub>4</sub>	8.14	1.70	0.10	1.55	0.22
29	<i>p</i> -(MeO) <sub>2</sub> C <sub>6</sub> H <sub>4</sub>	7.96	1.50	0.11	1.34	0.18
30	Me <sub>5</sub> C <sub>6</sub> H		1.84	0.12	1.54	0.17

<sup>a</sup> Measured with a stationary platinum microelectrode at 100 mV s<sup>-1</sup> at 25 °C. <sup>b</sup> From ref 33a. <sup>c</sup> From ref 33b. <sup>d</sup> From ref 33c. <sup>e</sup> Containing 0.10 M NaClO<sub>4</sub> as the supporting electrolyte. <sup>f</sup> Peak potential (V) relative to saturated NaCl SCE. <sup>g</sup> Containing 0.10 M Et<sub>4</sub>NClO<sub>4</sub>.

voltammetry (CV) of the series of substituted benzenes included in Table III was examined in both trifluoroacetic acid and acetonitrile solutions with a stationary platinum microelectrode at 25 °C, using 0.1 M tetraethylammonium perchlorate and sodium perchlorate, respectively, as supporting electrolytes. The cyclic voltammogram of hexaethylbenzene in trifluoroacetic acid shows both anodic and cathodic waves of roughly equal magnitude, but they are separated by more than the theoretical value of 57 mV expected for a reversible electrochemical couple. The cyclic voltammograms of the other arenes are also characterized by well-defined anodic waves, but no cathodic waves were observed on the reverse scan, even at high scan rates. The irreversible CV behavior suggests that the arene cation-radical formed on anodic oxidation is unstable, in accord with other electrochemical studies.<sup>31,32</sup>

The anodic peak potential  $E_p$  measured at a constant CV sweep rate is subject to large and systematic variations which parallel the vertical ionization potentials measured independently from the photoelectron spectra of various substituted benzenes.<sup>33</sup> Furthermore, the anodic peak potentials measured in trifluoroacetic acid are consistently less positive than those measured in acetonitrile by approximately 0.2 ± 0.1 V (i.e., under equivalent

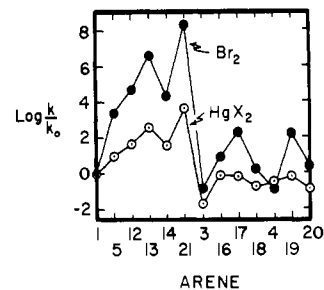


Figure 4. Variations in the relative reactivities of arenes in mercuration (○) and bromination (●). The substituted benzenes are identified by numbers in Table I.

conditions the arenes are more easily oxidized in trifluoroacetic acid relative to acetonitrile). The widths of the CV waves ( $E_p - E_{p/2}$ ) listed in Table III vary with the arenes, generally increasing with  $E_p$  and a solvent change from acetonitrile to trifluoroacetic acid.<sup>34</sup>

## Discussion

Halogenation and mercuration represent rather dissimilar processes for electrophilic aromatic substitution, as illustrated by the divergent trends in the relative reactivities ( $\log k/k_0$ ) of various arenes toward Br<sub>2</sub> and Hg(O<sub>2</sub>CCF<sub>3</sub>)<sub>2</sub> in Figure 4. Thus any mechanistic formulation of electrophilic aromatic substitution must first reconcile, in a quantitative way, such differences in arene reactivities imposed by the different electrophiles. Furthermore, if the formulation is to have any generality and predictive power, it must lead to the description of the activation process for electrophilic aromatic substitution in terms of experimentally identifiable concepts. Indeed there have been extensive efforts to develop linear free energy relationships from experimentally accessible models such as the  $\sigma^+$  constants from the solvolysis of cumyl chlorides,<sup>7</sup> the basicity constants for  $\sigma$  complexes of arenes with HF/BF<sub>3</sub><sup>11</sup> and for  $\pi$  complexes of arenes with HCl,<sup>12</sup> the ionization potentials of arenes from photoelectron spectroscopy,<sup>33</sup> and the proton affinities of arenes from ion cyclotron resonance spectroscopy.<sup>35</sup> However, no clear criterion has been developed as to what the linear free energy relationships actually represent, especially as to what the (Brønsted) slope should be.<sup>36</sup> Whenever a linear free energy relationship has been obtained for an electrophilic aromatic substitution, it has been discussed only in qualitative terms by either drawing on the similarity to the transition-state or to the ground-state properties of the reference process.<sup>37</sup>

We wish to approach electrophilic aromatic substitution in an entirely different way, which stems from the observation of the

(34) Nicholson, R. S.; Shain, I. *Anal. Chem.* **1964**, *36*, 706.

(35) (a) Aue, D. H.; Bowers, M. T. In "Gas Phase Ion Chemistry"; Bowers, M. T., Ed.; Academic Press: New York, 1979; Vol. 2, Chapter 9. (b) Kebabian, P. *Annu. Rev. Phys. Chem.* **1977**, *28*, 445. (c) Baldeschwieler, J. D.; Woodgate, S. S. *Acc. Chem. Res.* **1971**, *4*, 114.

(36) (a) The success of Brown  $\sigma^+$  constants for the linear free energy relations depends on simply replacing the unknown transition state for electrophilic aromatic substitution with a transition state for the solvolysis of substituted phenyldimethylcarbinyl chlorides, which it is generally thought to reflect the importance of the "carbonium ion type" of transition state. (b) The success of the linear free energy relationships with  $\sigma$  basicities<sup>37b</sup> as well as with the proton affinities<sup>37c</sup> depends on the similarity between the  $\sigma$  complex and the transition state. However, the slopes are dependent on the electrophile in an unaccountable manner. Therefore, there is no criterion on which to base their similarity. (c) The linear free energy relations with a wide range of  $I_D$ <sup>37d</sup> suggests the importance of electron transfer [Ar<sup>+</sup>] in the transition states. However, the same difficulties are applied as those above.

(37) (a) Brown  $\sigma^+$  constants.<sup>7</sup> (b) Basicity constants for  $\sigma$  complexes (ref 1g, l, m and 8; see also: Altschuler, L.; Berliner, E. *J. Am. Chem. Soc.* **1966**, *88*, 5837). (c) Basicity constants for  $\pi$  complexes.<sup>1c,l,m</sup> Note the correlations are usually poor. (d) Linear free energy relationship with  $I_D$ <sup>1k</sup> and Pederson, E. B.; Petersen, T. E.; Torrsell, K.; Lawesson, S.-O. *Tetrahedron* **1973**, *29*, 579. (e) Although the linear free energy relationship with the proton affinities has not been tested, the linear correlation between the proton affinities and  $\sigma^+$  constants (see: McKelvey, J. M.; Alexandratos, S.; Streiwieser, A., Jr.; Abboud, J.-L.-M.; Hehre, W. J. *J. Am. Chem. Soc.* **1976**, *98*, 244) indicates its applicability.

(31) For a discussion of the cyclic voltammetry of irreversible processes, see: Klingler, R. J.; Kochi, J. K. *J. Am. Chem. Soc.* **1980**, *102*, 4790.

(32) (a) Osa, T.; Yildiz, A.; Kuwana, T. *J. Am. Chem. Soc.* **1969**, *91*, 3994. (b) Bewick, A.; Edwards, G. J.; Mellor, J. M.; Pons, S. *J. Chem. Soc., Perkin Trans. 2* **1977**, 1952. (c) Parker, V. D.; Adams, R. N. *Tetrahedron Lett.* **1969**, *21*, 1721. (d) Evans, D. H. *Acc. Chem. Res.* **1977**, *10*, 313.

(33) (a) Reference 16 and references cited therein. (b) Watanabe, K.; Nakayama, T.; Mottl, J. J. *Quant. Spectrosc. Radiat. Transfer* **1962**, *2*, 369. (c) Kobayashi, T.; Nagakura, S. *Bull. Chem. Soc. Jpn.* **1974**, *47*, 2563.

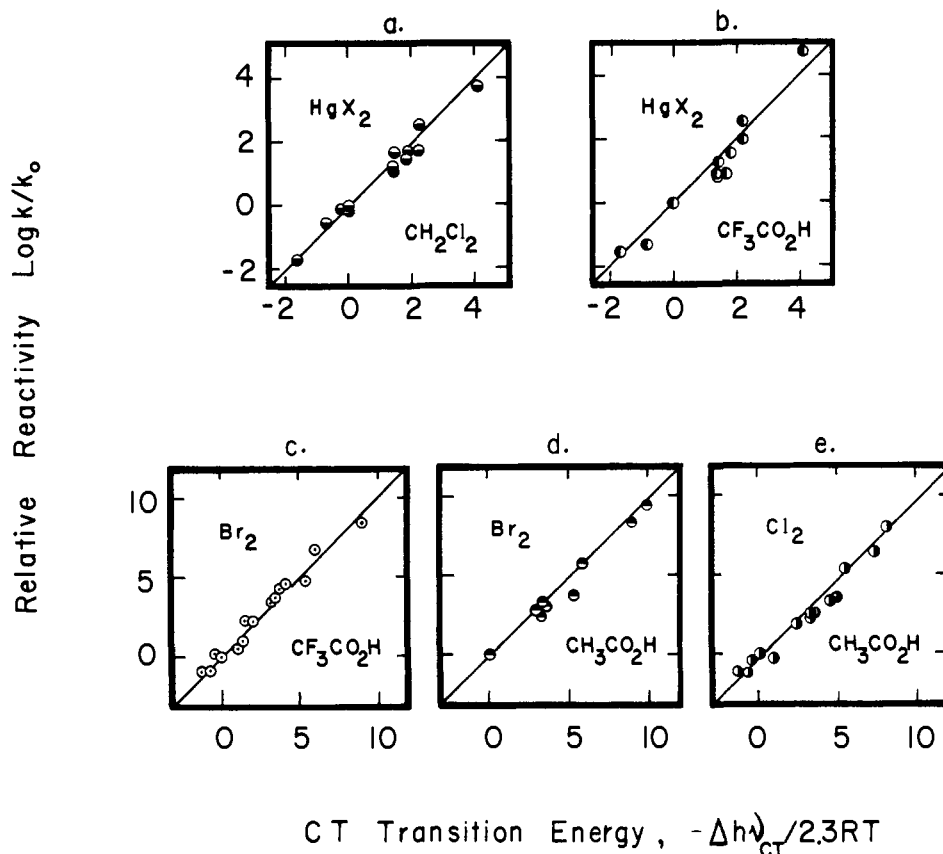


**Figure 5.** The correlation of the relative reactivities of arenes with the CT transition energies for (a)  $\text{Hg}(\text{O}_2\text{CCF}_3)_2$  in methylene chloride, (b)  $\text{Hg}(\text{O}_2\text{CCF}_3)_2$  in trifluoroacetic acid, (c)  $\text{Br}_2$  in trifluoroacetic acid, (d)  $\text{Br}_2$  in acetic acid, and (e)  $\text{Cl}_2$  in acetic acid. The lines are arbitrarily drawn with a slope of unity to emphasize the fit to eq 10.

transient charge-transfer (CT) bands when arenes are treated with electrophiles. In particular, we wish to show how the CT formulation provides the basis for unifying various electrophilic aromatic substitution processes by focussing on the properties of the CT excited state and the unique information provided by the CT transition energy.

**I. Charge-Transfer Formulation of Electrophilic Aromatic Substitution.** The relative reactivity of an arene in electrophilic aromatic substitution is represented by the activation free energy difference

$$\Delta G_r^* = -2.3RT \log k/k_0 \quad (8)$$

where the subscript *r* refers to changes relative to that of benzene, arbitrarily chosen as the reference arene. The CT transition energy  $h\nu_{\text{CT}}$  associated with an electrophile-arene pair can be evaluated by a similar comparative procedure, i.e.

$$\Delta h\nu_{\text{CT}} = h\nu_{\text{CT}} - h\nu_{\text{CT}}^0 \quad (9)$$

where  $h\nu_{\text{CT}}^0$  is the CT transition energy of the same electrophile with the benzene reference. In order to emphasize that  $\Delta h\nu_{\text{CT}}$  refers to a particular electrophile interacting with a family of substituted benzenes, it is designated as  $\xi_E$  and converted to a scale common with the rate constants, i.e.,  $\xi_E = \Delta h\nu_{\text{CT}}/2.3RT$ . Values of  $\xi_E$  for  $\text{Hg}(\text{O}_2\text{CCF}_3)_2$ ,  $\text{Br}_2$ , and  $\text{Cl}_2$  are obtained from the data in Tables I and II, and listed in Table IV for convenience. It is noteworthy that values of  $\xi_E$  for mercuric trifluoroacetate are uniformly smaller than those for either chlorine or bromine.<sup>38</sup>

**A. Correlation of the Relative Reactivities and the CT Transition Energies.** The direct relationship between the relative reactivities of various arenes in electrophilic substitution and the CT transition

**Table IV.** CT Transition Energies in the Interaction of Aromatic Compounds with Various Electrophiles<sup>a</sup>

aromatic compd <sup>b</sup> no.	$-\Delta I_D/$ $2.3RT$	relative CT transition energy, $\xi_E$			
		Hg- ( $\text{O}_2\text{CCF}_3$ ) <sub>2</sub> ( $\text{CH}_2\text{Cl}_2$ )	$\text{Br}_2$ ( $\text{CCl}_4$ )	$\text{Br}_2$ ( $\text{CF}_3\text{CO}_2\text{H}$ )	$\text{Cl}_2^c$ ( $\text{CCl}_4$ )
1	0	0	0	0	0
3	2.5	-1.7	-1.9	-1.4	(-1.4)
4	3.0	-0.8	-0.5	-0.8	(-0.8)
5	6.9	1.4	2.9	3.2	3.2
6	7.9	1.4	2.9	3.2	3.0
7	8.6	1.7	2.9	3.4	
8	9.1	1.4	2.9	3.4	3.2
9	9.1	1.7	3.2	3.2	3.2
10	9.3	1.4	2.9	3.2	2.4
11	14.2		10.0		10.5
12	11.3	2.2	5.4	5.4	4.9
13	11.3	2.2	5.9		5.4
14	13.4	1.9	3.2	3.7	4.6
15		1.9	3.9	3.9	4.4
16	6.8	-0.3	1.5	1.4	
17	6.8	0	0.8	1.5	
18	9.1	<0.5	-0.5	<1.0	(-0.5)
19	7.1	0	1.5	1.9	
20	9.5	<0.5	1.2	1.0	(1.0)
21	14.0	4.1	9.0		8.1
22			9.1		
23	19.9		9.3		7.3
24	23.3	11.8	16.2		14.9
25		10.1	15.4		

<sup>a</sup> See text. <sup>b</sup> Identified in Table I. <sup>c</sup> For the values in parentheses, see ref 38.

(38) Since the values of  $\xi_E$  for  $\text{Cl}_2$  are similar to those for  $\text{Br}_2$ , those values which are unavailable for  $\text{Cl}_2$  were taken to be the same as those for  $\text{Br}_2$  (in parentheses) in Table IV.

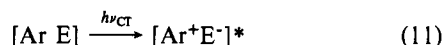
energies is shown in Figure 5. The remarkable linear correlations of the data apply equally well to mercuriation, to bromination, and to chlorination.<sup>39</sup> Moreover, the same relationship is applicable

in solvents as diverse as methylene chloride, acetic acid, and trifluoroacetic acid. Since every line in Figure 5 is arbitrarily drawn with a slope of unity,<sup>40</sup> if all the experimental points in Figure 5 were plotted in a single figure, they would all line on a single line. This corresponds to the linear free energy relationship given in eq 10, which is applicable to every electrophilic substitution process examined in this study.

$$\log k/k_0 = -\Delta h\nu_{CT}/2.3RT = \xi_E \quad (10)$$

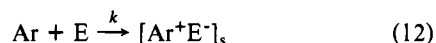
We now wish to inquire as to the origin of the remarkable linear correlations shown in Figure 5 and expressed by eq 10 and to discuss how it pertains to the activation process in electrophilic aromatic substitution.

**B. Nature of the CT Excited State and the Transition State for Electrophilic Aromatic Substitution.** For weak EDA complexes of the type described for the arene-electrophile pairs in this study, the spectral transition  $h\nu_{CT}$  represents an electronic excitation from the neutral ground state to the polar excited state, i.e.,<sup>17</sup> eq 11.



The asterisk identifies an excited ion pair with the same mean separation  $r_{DA}$  as that in the EDA complex. The nature of the CT excited state has been verified as the polar ion pair in eq 11, by applying spectroscopic methods with pulsed laser excitation.<sup>41</sup> Thus in arene complexes with  $\pi$  acceptors such as tetracyanobenzene and pyromellitic anhydride, the absorption spectrum of the excited EDA complex has been shown to consist of the superposition of the spectral bands of the aromatic donor cation  $Ar^+$  and the electron acceptor anion  $E^-$ .<sup>41,42</sup> In other words, the CT transition energy  $h\nu_{CT}$  represents the energetics of ion-pair formation, which indeed accords with the generalized Mulliken theory of charge transfer.<sup>17</sup>

Based on the striking correlations in Figure 5, we conclude that the formation of the ion pair in eq 11 is tantamount to the activation process for electrophilic aromatic substitution, i.e.,<sup>43</sup>



Taken further, we suggest that the ion pair  $[Ar^+E^-]$  is a reasonable approximation to the transition state for electrophilic aromatic substitution.<sup>45</sup> It should be noted, however, that the transition state is attained by an adiabatic process, whereas the CT excitation

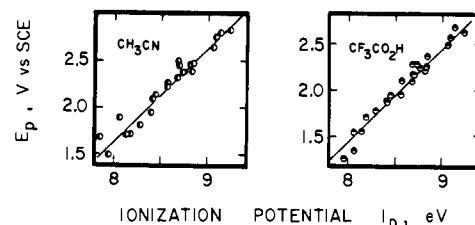


**Figure 6.** The correlation of the first vertical ionization potentials  $I_D$  of various arenes with the anodic peak potentials  $E_p$  in acetonitrile (left) and in trifluoroacetic acid (right). Note the lines are arbitrarily drawn with a slope of unity to emphasize the direct relationship.

represents a vertical (Franck-Condon) transition. As such, the CT excited ion pair involves minimal changes in solvation, which occurs only in a subsequent relaxation process. (For example, the relaxation from the Franck-Condon excited state to the equilibrium fluorescent state is associated with an extraordinarily large Stokes shift of 34 kcal mol<sup>-1</sup> for the tetracyanobenzene-toluene EDA complex in toluene.<sup>46</sup>) By contrast, the formation of the polar ion pair by a thermal activation must be accompanied by changes in solvation, as indicated by the subscript  $s$  in eq 12. In order to resolve this dilemma, we now consider the solvent effect in electrophilic aromatic substitution, especially in the context of the CT formulation.

**C. Solvent Effect.** Relatively large changes in solvation are expected to accompany electron transfer in eq 12, since the solvation of the neutral complex may be neglected in comparison with that of the ion pair.<sup>47</sup> By the comparative procedure used to develop eq 10, we need only to consider relative changes in the solvation of the aromatic cation, since the contributions from the electrophile moiety drop out by cancellation. Under these circumstances, the free energy change for solvation is represented by the difference between the gas-phase ionization potential



and the free energy change for oxidation in solution



of the arene, where the subscript  $s$  represents the solvated species. Unfortunately, the standard oxidation potential  $E^0$  is unknown for mononuclear aromatic compounds owing to their transient existence. However, we showed earlier that anodic peak potentials  $E_p$  from the cyclic voltammetry of irreversible electrode processes can be related directly to the activation free energy for heterogeneous electron transfer.<sup>31,48</sup> Indeed, Figure 6 shows that the ionization potentials correlate linearly with values of  $E_p$  in Table III, both in acetonitrile and in trifluoroacetic acid. Such a correlation of  $E_p$  and  $I_D$  (particularly with a slope of unity) supports the notion that solvation among a series of related benzene cations in acetonitrile and in trifluoroacetic acid is rather constant.<sup>49</sup> Although this conclusion must be tempered somewhat by the indirect measure of arene oxidation in solution, the same result has been proved with various polynuclear aromatic compounds,

(39) The values of  $\xi_E$  for  $Br_2$  were taken from those in  $CF_3CO_2H$  when they were available. Note: the values of  $\xi_E$  for  $Br_2$  obtained from the data in  $CCl_4$  are parallel to those in  $CF_3CO_2H$  with the slope of unity.<sup>16</sup> Thus, the values of  $\xi_E$  are independent of the solvent.

(40) Note 1 eV = 23.06 kcal mol<sup>-1</sup>.

(41) (a) Mataga, N.; Ottolenghi, M. In "Molecular Association"; Foster, R., Ed.; Academic Press: New York, 1979; Vol. 2, p 31. (b) Ottolenghi, M. *Acc. Chem. Res.* **1973**, *6*, 153. (c) Potashnik, R.; Ottolenghi, M. *Chem. Phys. Lett.* **1970**, *6*, 525. (d) Masuhara, H.; Mataga, N. *Ibid.* **1970**, *6*, 608. (e) Masuhara, H.; Mataga, N. *Bull. Chem. Soc. Jpn.* **1972**, *45*, 43. (f) Masuhara, H.; Tsujino, N.; Mataga, N. *Ibid.* **1973**, *46*, 1088. (g) Kobayashi, T.; Matsumoto, S.; Nagakura, S. *Chem. Lett.* **1974**, 235.

(42) The equivalence of the electrophiles such as  $Hg(O_2CCF_3)_2$ ,  $Br_2$ , and  $Cl_2$  and the  $\pi$  acceptors such as tetracyanobenzene and quinones in CT interactions has been shown.<sup>16</sup>

(43) (a) In more rigorous terms, eq 10 states that arenes are subjected to the same perturbations in electrophilic aromatic substitution as in CT transition, when they are evaluated relative to the benzene reference. The absolute magnitudes of the perturbations are not evaluated directly. (b) It is not germane to this discussion whether the EDA complex can or cannot be proved to lie along the reaction coordinate as an intermediate in electrophilic aromatic substitution. For a discussion of this point see ref 44. (c) Since the formation constants of these EDA complex are uniformly small ( $K < 1 M^{-1}$ ), there is essentially no difference in the energetics derived from the EDA complex or from the separated arene and electrophile.

(44) Fukuzumi, S.; Kochi, J. K. *J. Am. Chem.* **1980**, *102*, 2141. Fukuzumi, S.; Mochida, K.; Kochi, J. K. *Ibid.* **1979**, *101*, 5961.

(45) This statement is especially applicable when relative changes are considered (see ref 43). In the comparative procedure used to develop eq 10, factors which are common to the arene and to the reference (benzene) are cancelled out. Thus the validity of absolute comparisons depend on whether relative changes accurately reflect absolute changes as well.

(46) These experiments were verified (using a pulsed nitrogen laser excitation) as a time-dependent (1–100 ns) red shift of the fluorescence of the excited TCNB-toluene EDA complex, which directly reflects the solvent reorientation. Egawa, K.; Nakashima, N.; Mataga, N.; Yamanaka, C. *Chem. Phys. Lett.* **1971**, *8*, 108; *Bull. Chem. Soc. Jpn.* **1971**, *44*, 3287.

(47) The free energy of solution of neutral arenes has been evaluated as 1–2 kcal mol<sup>-1</sup> from solubility measurements in  $CH_2Cl_2$  and in  $CCl_4$ . (Lofti, M.; Roberts, R. M. G. *Tetrahedron* **1979**, *35*, 2137.) For other neutral molecules, see: Ben-Naim, A.; Wilf, J.; Yaacobi, M. *J. Phys. Chem.* **1973**, *77*, 95. Wilhelm, E.; Battino, R.; Wilcock, R. J. *Chem. Rev.* **1977**, *77*, 220.

(48) Klingler, R. J.; Kochi, J. K. *J. Phys. Chem.* **1981**, *85*, 1731.

(49) A similar correlation between the polarographic oxidation half-wave potentials and the ionization potential has been reported, and relatively small changes in the solvation energy are found in a variety of organic compounds. (Miller, L. L.; Nordblom, G. D.; Mayeda, E. A. *J. Org. Chem.* **1972**, *37*, 916 and references cited therein.)

for which  $E^0$  can be measured.<sup>50,51</sup> Thus by taking the solvation of arene cations to be relatively constant in trifluoroacetic acid and in acetonitrile, it follows that the vertical and adiabatic ion pairs in eq 11 and 12, respectively, are evaluated to be equivalent by the comparative procedure used in eq 10. It is noteworthy that the polar ion pair  $[\text{Ar}^+\text{E}^-]$ , when taken as a model for the transition state of electrophilic aromatic substitution, does correctly account for an otherwise inexplicable lack of sensitivity to solvent effects of the relative reactivities of various arenes,<sup>8</sup> despite a strong correlation with the  $\sigma^+$  parameter.

The *absolute* rates of electrophilic aromatic substitution also accord with ion-pair solvation. For example, the solvation energy of aromatic cations in trifluoroacetic acid is larger than that in acetonitrile by approximately 4.6 kcal mol<sup>-1</sup>, which corresponds to the difference in  $E_p$  in these solvents (see Table IV). The second-order rate constant for the chlorination of benzene in trifluoroacetic acid of  $k = 7 \times 10^{-3} \text{ M}^{-1} \text{ s}^{-1}$  at 25 °C is 1700 times larger than that in acetonitrile.<sup>52</sup> This rate enhancement is equivalent to a decrease of the activation free energy of 4.4 kcal mol<sup>-1</sup>, which corresponds well with the difference in solvation energy mentioned above. Although such an agreement may be fortuitous, it nonetheless underscores the importance of solvation in considering the solvent effects on the *absolute* rates of electrophilic aromatic substitution.<sup>53,54</sup>

**II. Significance of the CT Formulation to Other Linear Free Energy Relationships.** The charge-transfer formulation of electrophilic aromatic substitution leads to the conception of the transition state as the ion pair.<sup>55</sup> As such, we now wish to show how the CT formulation relates to previous linear free energy relationships which have been developed for electrophilic aromatic substitution.

First, let us consider the well known correlation based on Brown's  $\sigma^+$  substituent constants,<sup>56</sup> viz., eq 15. Since the sen-

$$\log k/k_0 = \rho\sigma^+ \quad (15)$$

(50) (a) Case, B. In "Reactions of Molecules at Electrodes"; Hush, N. S., Ed.; Wiley-Interscience: New York, 1971; p 125. (b) Peover, M. E. *Electroanal. Chem.* **1967**, 2, 1.

(51) (a) The solvation energies of aromatic cations  $\Delta G^{\ddagger}$  have been calculated by the relationship<sup>50</sup>  $-\Delta G^{\ddagger} = I_D - \mathcal{F}(E^0 - C)$ , where  $\Delta G^{\ddagger}$  is the change in the solvation energy relative to the neutral arene,<sup>47</sup>  $\mathcal{F}$  is the Faraday constant, and  $E^0$  is the standard oxidation potential of the arene.  $C$  is a constant (4.70 V vs. Ag/Ag<sup>+</sup> at 25 °C), which includes the potential of the reference electrode on the absolute scales, together with liquid junction potentials. The values of  $\Delta G^{\ddagger}$  for anthracene, phenanthrene, chrysene, pyrene, triphenylene, and tetraphenylene are almost constant at  $38 \pm 1$  kcal mol<sup>-1</sup> in acetonitrile.<sup>50</sup> (b) Since the accurate ionization potentials were not available for all the compounds when the values of  $\Delta G^{\ddagger}$  was first evaluated in ref 50, we recalculated  $-\Delta G^{\ddagger}$  by using the recent data for the ionization potentials of these compounds. (Herndon, W. C. *J. Am. Chem. Soc.* **1976**, *98*, 887.) The results are as follows: anthracene, 40.1 kcal mol<sup>-1</sup>; phenanthrene, 38.0 kcal mol<sup>-1</sup>; chrysene, 37.3 kcal mol<sup>-1</sup>; pyrene, 36.6 kcal mol<sup>-1</sup>; triphenylene, 38.2 kcal mol<sup>-1</sup>; tetracene, 36.6 kcal mol<sup>-1</sup>. The average value is  $37.8 \pm 1.3$  kcal mol<sup>-1</sup>.

(52) The rate constant for the chlorination of benzene is evaluated as  $4.1 \times 10^{-6} \text{ M}^{-1} \text{ s}^{-1}$  in CH<sub>3</sub>CN at 25 °C on the basis of the rate constant of toluene ( $1.5 \times 10^{-3} \text{ M}^{-1} \text{ s}^{-1}$ )<sup>15</sup> and the ratio of the reactivity of toluene to benzene (360) in Table II.

(53) (a) The rates of electrophilic aromatic substitution are generally recognized to increase with the polarity of the medium. (see: Andrews, L. J.; Keefer, R. M. *J. Am. Chem. Soc.* **1957**, *79*, 1412, 5169. Seshadri, K. V.; Ganesan, R. Z. *Phys. Chem. (Wiesbaden)* **1968**, *62*, 29.) However, trifluoroacetic acid, which is less polar than acetonitrile, is capable of specific solvation to aromatic cations.<sup>27b</sup> (b) At this juncture, further quantitative evaluations of solvent effects are limited by the absence of data relating to the solvation of aromatic cations.

(54) It is noteworthy that the Stokes shift of 34 kcal mol<sup>-1</sup> for the fluorescence of the toluene-TCNB complex<sup>46</sup> is about the same as the solvation energy of aromatic cation (38 kcal mol<sup>-1</sup>).<sup>51b</sup> When the solvation of the TCNB anion and the difference of the solvent are taken into account, the solvation in the equilibrium fluorescent state may be approximated by the sum of the solvation of each cation and anion. Thus, the Stokes shift in the fluorescence of the excited EDA complexes could provide further insight into the solvent effects in the electrophilic aromatic substitutions on the absolute scale.

(55) We do not intend to convey the notion that the transition state and the CT excited ion pair are the same, but only that one serves as a model for the other. See ref 43.

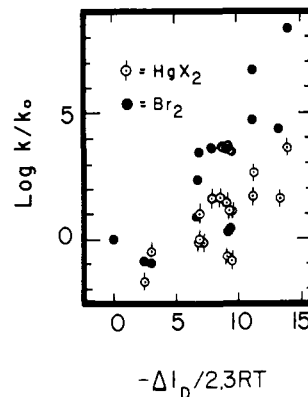


Figure 7. The variation of the relative reactivities in bromination (●) and mercuration (○) with the relative ionization potentials of the arenes.

sitivity factor  $\rho$  in eq 15 has been subjected to various physical interpretations, our primary task is to derive  $\rho$  from the CT data. It has been shown for a series of electrophiles and  $\pi$  acceptors that the CT transition energies  $h\nu_{CT}$  vary linearly with the ionization potential  $I_D$  of the arene donor.<sup>16</sup> The relative change, as evaluated by the comparative procedure (compare eq 10), is given by eq 16, where the slopes  $\alpha_E$  are measures of the electrophile

$$\Delta h\nu_{CT}/\Delta I_D = \alpha_E \quad (16)$$

or  $\pi$  acceptors—varying from  $\sim 0.3$  for  $\text{Hg}(\text{O}_2\text{CCF}_3)_2$ , 0.6 for tetracyanobenzene, 0.6 for  $\text{Cl}_2$ , 0.7 for  $\text{Br}_2$ , 0.7 for maleic anhydride, and 0.8 for tetracyanoethylene, up to 1.0 for chloranil. The values of  $\alpha_E$  never exceed unity. The linear free energy relationship between  $I_D$  and  $\sigma^+$  has been established for roughly 50 mono- and disubstituted benzenes as<sup>57</sup>

$$\Delta I_D = -20.4\sigma^+ \quad (17)$$

The combination of eq 10, 16, and 17 yields<sup>58</sup>

$$\log k/k_0 = -16\alpha_E\sigma^+ \quad (18)$$

In other words, the electrophile-dependent value of  $\rho$  in eq 15 is directly related to the slope of the correlation of  $h\nu_{CT}$  with  $I_D$ , i.e.

$$\rho = -16\alpha_E \quad (19)$$

Since  $0 < \alpha_E < 1$ , eq 19 predicts that  $\rho$  will not exceed a value of 16. Indeed we are unaware of reports in the extant literature of  $|\rho| > 16$  for any electrophilic aromatic substitution. Furthermore, the  $\rho$  values for bromination ( $\rho = -12.1$ ) and for chlorination ( $\rho = -10.0$ ) are readily obtained from the CT data with the aid of eq 19. Thus by using the values of  $\alpha_E$  for the bromine complexes and for the chlorine complexes (vide supra), we calculated the  $\rho$  values for bromination and chlorination from eq 19 to be  $\rho = -11$  and  $\rho = -9.6$ , respectively. Similarly, the  $\rho$  value for mercuration of  $-5.7$  agrees well with the calculated

(56) Although  $\sigma^+$  for many substituents is effectively constant over a wide range in the variation of  $\rho$  in various electrophilic aromatic substitutions, there are substituents such as (F, Cl, and Br) in which there is a considerable variation in  $\sigma^+$  with changes in  $\rho$ . See: Knowles, J. R.; Norman, R. O. C.; Radda, G. K. *J. Chem. Soc.* **1960**, 4885. van Bekkum, H.; Verkade, P. E.; Wepster, B. M. *Recl. Trav. Chim. Pays-Bas* **1959**, *78*, 815. The inconsistency of  $\sigma^+$  constants necessitated the introduction of multiparameter extensions to the Hammett equation.<sup>7b</sup>

(57) (a) Gibson, H. W. *Can. J. Chem.* **1973**, *51*, 3065. (b) Thompson, M.; Hewitt, P. A.; Wooliscroft, D. S. In "Handbook of X-ray and Ultraviolet Photoelectron Spectroscopy"; Briggs, D., Ed.; William Clowes & Sons Limited: London, 1978; Chapter 10, p 344. (c) In eq 17,<sup>57a</sup>  $\sigma^+$  values were used since they include contributions from both the resonance and inductive effects. For disubstituted benzenes, the summation of  $\sigma^+$  values are used. The correlation coefficient is 0.967, excluding phenols, bromides, and iodides.<sup>57a</sup> The correlation including only the monosubstituted benzenes gives  $\Delta I_D = -22.6\sigma^+$  (15 monosubstituted benzenes). We examined the correlation by including six other monosubstituted benzenes (F, CF<sub>3</sub>, SMe, Ph, NHCO-CH<sub>3</sub>, and CO<sub>2</sub>H) and using the more recent literature values of  $I_D$ .<sup>16</sup> The correlation is  $\Delta I_D = -20.6\sigma^+$ . Thus, the proportionality constant in the correlation between  $\Delta I_D$  and  $\sigma^+$  is rather constant between  $-20.4$  and  $-22.6$ , irrespective of the source of the data.

(58) The transformation includes a factor of  $0.733 = 1/2.3RT$  at 298 K when  $\Delta I_D$  is expressed in units of kcal mol<sup>-1</sup>.



Table V. Isomer Distribution in the Electrophilic Substitution of Monosubstituted Benzenes

Ph-X <sup>a</sup> X	$\sigma_P^{\circ c}$	$I_D,^d$ eV	Hg(O <sub>2</sub> CCF <sub>3</sub> ) <sub>2</sub> <sup>l</sup>			Br <sub>2</sub> <sup>l</sup>			Tl(O <sub>2</sub> CCF <sub>3</sub> ) <sub>3</sub> <sup>l</sup>			nitration <sup>r</sup>		
			no.	p	m	no.	p	m	no.	p	m	no.	p	m
F	0.15	9.19 <sup>e</sup>	(1)	72	0				(22)	95	0	(30) <sup>s</sup>	91	0
Cl	0.24	9.08	(2)	73	0				(23)	97	1	(31) <sup>t</sup>	70	1
Br	0.27	9.05	(3)	80	2				(24)	97	2	(32) <sup>t</sup>	62	1
I	0.28	8.67 <sup>e</sup>										(33) <sup>u</sup>	64	0
SMe	0.06	8.07 <sup>f</sup>				(10) <sup>n</sup>	94	0						
Ph	0.05	8.32 <sup>g</sup>				(11) <sup>o</sup>	98	0						
NHAc	0	8.47 <sup>h</sup>	(4) <sup>m</sup>	100	0	(12) <sup>p</sup>	100	0				(34) <sup>w</sup>	80	0
Me	-0.14	8.82	(5)	73	6	(13)	82	0	(25)	86	5	(35)	40	0
Et	-0.13	8.76	(6)	94	4	(14)	87	0	(26)	97	2	(36) <sup>s</sup>	51	3
<i>i</i> -Pr	-0.13	8.69	(7)	94	5	(15)	92	0	(27)	98	2	(37) <sup>s</sup>	68	5
<i>t</i> -Bu	-0.15	8.68	(8)	92	8	(16)	100	0	(28)	100	0	(38) <sup>s</sup>	83	7
OMe	-0.12	8.39	(9)	81	0	(17) <sup>o</sup>	98	0	(29)	92	0	(39) <sup>x</sup>	67	2
OH	-0.22	8.73 <sup>i</sup>				(18) <sup>o</sup>	100	0						

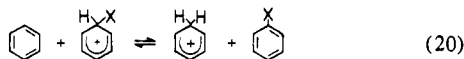
  

Ph-Y <sup>b</sup> Y	$\sigma_P^{\circ c}$	$I_D,^e$ eV	F <sub>2</sub> <sup>q</sup>			nitration		
			no.	p	m	no.	p	m
CN	0.71	9.72 <sup>i</sup>	(19)	13	62	(40)	2	81
NO <sub>2</sub>	0.81	9.93 <sup>i</sup>	(20)	11	80	(41)	0	93
CF <sub>3</sub>	0.54	9.70 <sup>e</sup>	(21)	20	64	(42) <sup>y</sup>	3	91
CO <sub>2</sub> H	0.44	9.73 <sup>j</sup>				(43)	1	80
CO <sub>2</sub> Me	0.44	9.35 <sup>j</sup>				(44) <sup>t</sup>	4	72
CHO	0.47	9.59 <sup>k</sup>				(45)	9	72
COCH <sub>3</sub>	0.47	9.37 <sup>i</sup>				(46) <sup>y</sup>	1	72

<sup>a</sup> X = electron-releasing substituent with  $I_D < 9.23$  eV (C<sub>6</sub>H<sub>6</sub>). <sup>b</sup> Y = electron-withdrawing substituent with  $I_D > 9.23$  eV. <sup>c</sup> Hammett constants for inductive effect from ref 74. <sup>d</sup> See Table I. <sup>e</sup> From ref 80a. <sup>f</sup> From ref 80b. <sup>g</sup> From ref 80c. <sup>h</sup> From ref 80d. <sup>i</sup> From ref 33c. <sup>j</sup> From ref 80e. <sup>k</sup> From ref 80f. <sup>l</sup> In CF<sub>3</sub>CO<sub>2</sub>H from ref 20. <sup>m</sup> Mercuration by Hg(OAc)<sub>2</sub> in AcOH from ref 1 g. <sup>n</sup> In CCl<sub>4</sub> at 110 °C from ref 69a. <sup>o</sup> In AcOH from ref 69b. <sup>p</sup> In AcOH from ref 1 g. <sup>q</sup> In FClCl<sub>3</sub> at -78 °C from ref 70. <sup>r</sup> From ref 1e. <sup>s</sup> From ref 56. <sup>t</sup> From ref 71a. <sup>u</sup> From ref 70b. <sup>w</sup> From ref 1h. <sup>x</sup> See ref 72. <sup>y</sup> From ref 71c.

value of -5 based on  $\alpha_E = 0.3$ .<sup>59</sup> Thus the absolute values of  $\rho$ , otherwise unpredictable, can be independently evaluated for various electrophiles by the use of eq 19.<sup>60</sup>

Other linear free energy relationships can be considered in a similar light with the CT data. For example, the relative proton affinity  $\Delta PA$  of arenes in the gas phase, which is obtained from the isodesmic process,<sup>61</sup> eq 20, is a linear function of  $\sigma^+$  constants



for para substituents:<sup>61</sup>  $\Delta PA = -21.4\sigma^+$ . Since the proton affinities and the ionization potentials are known to be linearly correlated with a slope of unity,<sup>62</sup> the CT correlation in eq 10 of the relative reactivities in electrophilic aromatic substitution is established through eq 16. The same applies to the correlation of the  $\sigma$  basicity of arenes, since it is also linearly related to the ionization potential of the arenes.<sup>63</sup> Furthermore, of the many theoretical indices which have been proposed, the localization energy which is proportional to the ionization potential ( $L_r^+ =$

$-1.06I_D + 21.7$ ) has been found to be the most fundamental and reliable measure of arene reactivity in electrophilic substitution.<sup>64</sup>

With the relationships to previous linear free energy correlations thus established, the physical basis for the CT formulation in eq 10 can now be developed. According to Mulliken theory,<sup>17</sup> the energy change associated with the vertical (Franck-Condon) transition in eq 11 is given by eq 21, where  $E_A$  is the vertical

$$h\nu_{CT} = I_D - E_A + \omega \quad (21)$$

electron affinity of the electrophile. The interaction energy  $\omega$  within the excited ion pair is given to first order by the Coulombic work term,  $e^2/r_{DA}$ . If the mean separation  $r_{DA}$  were to remain constant in a series of arenes, the relative reactivities in eq 10 should be proportional to the differences in the ionization potentials, i.e.,  $\log k/k_0 = -\Delta I_D/2.3RT$ , since  $\Delta h\nu_{CT}$  would simply be equal to  $\Delta I_D$ , according to eq 21. A plot of the values of  $\Delta I_D/2.3RT$  listed in Table IV against the relative reactivities of arenes in bromination and mercuration is shown in Figure 7. The absence of any clear correlation indicates that the intrinsic donor abilities of the arenes (i.e.,  $\Delta I_D$ ) are alone insufficient to account for the differences in arene reactivities in mercuration and bromination. Thus the linear correlation of  $\log k/k_0$  with  $\Delta h\nu_{CT}$  in Figure 5 indicates that the interaction energy  $\omega$  is not constant. In order to determine the effects of a varying  $\omega$ , we differentiate eq 21 to yield the slope of the correlation of  $h\nu_{CT}$  and  $I_D$  as

$$\alpha_E = \frac{\partial(h\nu_{CT})}{\partial I_D} = 1 + \frac{\partial\omega}{\partial I_D} \quad (22)$$

Since the interaction between Ar<sup>+</sup> and E<sup>-</sup> is attractive, the work term  $\omega$  is negative and increases with the mean separation  $r_{DA}$ . Such an increase in  $r_{DA}$  is generally accompanied by a decrease in  $I_D$  of the substituted benzenes.<sup>16</sup> As a result, the term  $\partial\omega/\partial I_D$  in eq 22 is negative and leads to values of  $\alpha_E$  less than unity. Since the work term  $\omega$  in eq 21 must also be affected by the electrophile moiety E<sup>-</sup>, the term  $\partial\omega/\partial I_D$  is also dependent on the electrophile, as observed by the various values of  $\alpha_E$ . (For a further discussion of the changes in  $r_{DA}$  in the CT interactions with other donors,

(59) For mercuration by Hg(O<sub>2</sub>CCF<sub>3</sub>)<sub>2</sub>, the  $\rho$  value is reported as -5.7.<sup>20b</sup> For the Hg(O<sub>2</sub>CCF<sub>3</sub>)<sub>2</sub> complexes, the correlation between  $\Delta h\nu_{CT}$  and  $\Delta I_D$  is rather poor.<sup>16</sup> The  $\alpha_E$  value for monosubstituted benzenes is 0.294 with a correlation coefficient of 0.83. However, the  $\alpha_E$  value including polysubstituted benzenes is 0.500 with a correlation coefficient of 0.93. Thus the  $\rho$  values evaluated by eq 19 may be as low as -8.

(60) It should be noted that the use of eq 19 relies on the linear relationships in eq 16 and 17. When the linear correlation of  $h\nu_{CT}$  with  $I_D$  in eq 16 is poor (especially with the deviation of  $\alpha_E$  from unity<sup>59</sup>), eq 19 is of only qualitative significance.

(61) McKelvey, J. M.; Alexandratos, S.; Streitwieser, A., Jr.; Abboud, J.-L. M.; Hehre, W. J. *J. Am. Chem. Soc.* 1976, 98, 244. The linear relationship includes only para substituents (correlation coefficient 0.971) for the comparison with eq 17.<sup>57c</sup> The inclusion of meta substituents gives essentially the same result:  $\Delta E = -22.8\sigma^+ + 0.4$ .

(62) The proton affinities and the ionization potentials are correlated with the slope of unity when the same units are used, i.e.,  $\Delta E$  (kcal mol<sup>-1</sup>) = -23.1 $I_D$  (eV) + constant.

(63) (a) The relative  $\sigma$  basicities  $\log K/K_0$  using benzene as the reference<sup>11</sup> are correlated with the ionization potentials as  $\log K/K_0 = -6.7I_D + 62$  with a correlation coefficient of only 0.87. The correlation is better with  $h\nu_{CT}$  for the bromine complexes in Table II:  $\log K/K_0 = -13.6h\nu_{CT} + 59$  with a correlation coefficient of 0.96. Since the slope of the latter is close to unity (-0.80), the stabilities of these  $\sigma$  complexes track the CT excited state. (b) The correlation of the  $\pi$  complexes is poor; see ref 37c.

(64) Streitwieser, A., Jr.; Mowery, P. C.; Jesaitis, R. G.; Lewis, A. J. *Am. Chem. Soc.* 1970, 92, 6529. We used the values of  $I_D$  in ref 51b.

the reader is referred to ref 65.) Thus the successful unification of  $\rho$  from the linear free energy relationship and  $\alpha_E$  from the CT interaction underscores the similarity between the transition state for electrophilic aromatic substitution and excited ion-pair state in eq 11.<sup>66</sup>

The CT formulation of electrophilic aromatic substitution provides a physical representation of the transition state in terms of the ion pair  $[Ar^+E^-]$ . If such a formulation has any validity, the ion pair should also provide insight into the isomer distribution among the products, which is a well-considered aspect of the mechanism.<sup>1</sup> Indeed, Perrin in his earlier consideration of electron transfer during electrophilic nitration cited the relationship between positional reactivity and the HOMO spin densities in the phenanthrene and triphenylene cations.<sup>67</sup> Earlier, the substitution patterns for a variety of other electrophilic substitutions had been related to the ESR hyperfine coupling constants of the cations of various aromatic substrates.<sup>68</sup> The theoretical basis for such considerations was laid earlier.<sup>14</sup>

### III. Ion-Pair Collapse and the Isomeric Product Distribution.

The various isomer distributions among meta and para products which have been reported for the mercuration, halogenation, thallation, and nitration of monosubstituted benzenes are summarized in Table V.<sup>69-72</sup> The isomer distributions have been separated into two groups according to whether para products (Ph-X) or meta products (Ph-Y) predominate. Such directive effects of the substituents X and Y have been commonly rationalized on the basis of inductive, resonance, and steric effects, the particular combination being somewhat arbitrarily chosen.<sup>73</sup> For example, the halogens, F, Cl, Br, and I are classified as electron-withdrawing substituents by their values of the Hammett constants on the  $\sigma_p^0$  scale<sup>74</sup> and on the basis of the lower reactivity of the halobenzenes (compare Tables I and II). Nevertheless, they yield predominantly para isomers like their more reactive counterparts with X = alkyl, hydroxy, etc. Such abnormalities of the halobenzenes have been troublesome to rationalize and have led to rather unsatisfactory ad hoc explanations.<sup>75</sup>

The polar ion-pair state  $[Ar^+E^-]$  as a model for the transition state avoids the ambiguous situation of reconciling reactivities and

Scheme I

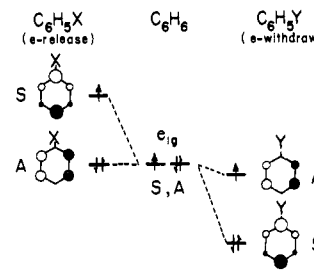


Chart I

substituent	ionization potential	isomer distribution
X (e release)	PhX < PhH	para > ortho >> meta
Y (e withdraw)	PhY > PhH	meta > ortho >> para

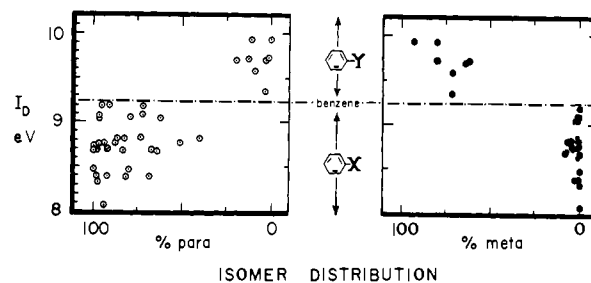
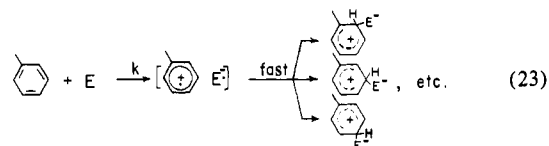


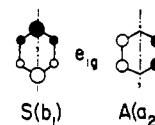
Figure 8. The product distribution among para isomers (left) and meta isomers (right) derived from monosubstituted benzenes with electron-releasing (X) and electron-withdrawing (Y) substituents, as indicated by the values of the ionization potential relative to that of benzene (9.23 eV) in Table V. Note that the halogens F, Cl, Br, and I are X substituents.

directive effects,<sup>76</sup> by separating the rate-determining step from the product-forming step. Thus the rate-limiting activation process is represented by the formation of the ion pair as described in the foregoing sections, and the product distribution is determined during the subsequent collapse of the ion pair, e.g.,<sup>77</sup> eq 23. Indeed



the ion pair is prepared for bonding in eq 23 by having the unpaired electrons located at the union centers, and hence they can be coupled to form the new bond.<sup>77</sup> Under these circumstances, the most probable course for the collapse of  $[Ar^+E^-]$  would be at the ring carbons of highest odd-electron spin density.

In the benzene cation, the unpaired electron lies in the degenerate  $e_{1g}$  HOMO's, labeled S (for symmetric  $b_1$ ) and A (for antisymmetric  $a_2$ ) below.<sup>78</sup> The spin density distributions for the odd electron in the benzene cation for these levels are



(76) For a succinct statement of the problem, see ref 67a. See, however: Santiago, C.; Houk, K. N.; Perrin, C. L. *J. Am. Chem. Soc.* 1979, 101, 1337.

(77) (a) Collapse of the ion pair is most likely to occur directly to the isomeric  $\sigma$  complexes. The subsequent step(s) leading to proton loss would then be the same as that involved in the conventional mechanisms. (b) In the recent theoretical study by Shaik (Shaik, S. S. *J. Am. Chem. Soc.* 1981, 103, 3692), the importance of the configuration ( $D^+A^-$ ) in the transition state has been emphasized whenever at least one of the reactants is a closed-shell molecule.

(78) Bowers, K. W. In "Radical Ions"; Kaiser, E. T., Kevan, L., Eds.; Interscience: New York, 1968; Chapter 5.

(65) Fukuzumi, S.; Kochi, J. K. *J. Phys. Chem.* 1980, 84, 608, 617; *J. Am. Chem. Soc.* 1981, 103, 2783.

(66) In ref 61, the authors state, "The difference in  $\rho$  no doubt stems both from solvent participation and from the fact that substituent effects may be only partially developed in the transition states for aromatic substitution compared to those in protonated species". From this study, the difference in  $\rho$  stems from changes in  $r_{DA}$  for the interactions between  $Ar^+$  and  $E^-$  in the ion pair, and solvents have essentially no effect on variations in  $\rho$ .

(67) (a) Perrin, C. L. *J. Am. Chem. Soc.* 1977, 99, 5516. (b) Electron transfer as proposed by Perrin is an outer-sphere process and as such differs fundamentally from the CT formulation in this study. The criticism of the outer-sphere mechanism in ref 70 does not apply to the CT formulation. See also Coombes, R. In "Comprehensive Organic Chemistry"; Sutherland, I. O., Ed.; Pergamon Press: Oxford, 1979, Vol. 2, p 309. Ebersson, L.; Jönsson, L.; Radner, F. *Acta Chem. Scand.* 1978, B32, 749. Coombes, R. G.; Golding, J. G.; Hadjigeorgiou, P. *J. Chem. Soc., Perkin Trans. 2* 1979, 1451. For a description of the differences between outer-sphere and inner-sphere electron transfer processes see: Fukuzumi, S.; Wong, C. L.; Kochi, J. K. *J. Am. Chem. Soc.* 1980, 102, 2928.

(68) See Pederson et al. in ref 37d.

(69) (a) Boicelli, A. C.; Danieli, R.; Mangini, A.; Ricci, A.; Pirazzini, G. *J. Chem. Soc., Perkin Trans. 2* 1974, 1343. (b) Stock, L. M.; Baker, F. W. *J. Am. Chem. Soc.* 1962, 84, 1661.

(70) Cacace, F.; Giacomello, P.; Wolf, A. P. *J. Am. Chem. Soc.* 1980, 102, 3511.

(71) (a) Brown, H. C.; McGary, C. W., Jr. *J. Am. Chem. Soc.* 1955, 77, 2300 and references cited therein. (b) Olah, G. A.; Kuhn, S. J.; Flood, S. H. *Ibid.* 1961, 83, 4571. (c) Hoggett, J. G.; Moodie, R. B.; Penton, J. R.; Schofield, K. "Nitration and Aromatic Reactivity"; Cambridge University Press: Cambridge, 1971.

(72) The values for the nitration of anisole were taken from ref 1e. However, the value of para isomer may not be accurate since it was shown to be dependent on the concentration of the sulfuric acid added to the system. (Barnett, J. W.; Moodie, R. B.; Schofield, K.; Weston, J. B. *J. Chem. Soc., Perkin Trans. 2* 1977, 248.)

(73) For an excellent summary of the earlier literature, see: Ingold, C. K. "Structure and Mechanism in Organic Chemistry", 2nd ed.; Cornell University Press: Ithaca, NY, 1969; Chapter 6.

(74) Wold, S.; Sjöström, M. In ref 7b, Chapter 1, p 25.

(75) For example, see p 55 in ref 1h.

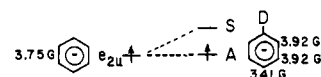
which leads overall to a spin density of one-sixth at each carbon center. The symmetric orbital has a large spin density at the 1- and 4-positions, where the antisymmetric orbital has a node.

The introduction of a substituent into benzene serves to remove the degeneracy of the symmetric and the antisymmetric orbitals—the electron-releasing substituent X leading to a raising of S and the electron-withdrawing substituent Y lowering S, as in the energy level diagram shown in Scheme I. This assignment has been indeed confirmed by the analysis of the electron spin resonance (ESR) spectra of various aromatic ion radicals, as described in detail in the Experimental Section. As a result, it is important to note that the spin densities at the para and the meta positions of aromatic cations differ markedly, depending on whether the substituent is X or Y. In Ph-X, the HOMO is S and the increased spin density in the para position is at the expense of a decreased spin density in the meta position. In Ph-Y, the HOMO is A and the converse would apply.

In order to utilize these spin densities for the prediction of the isomer distributions, we must classify the substituents as either X or Y. However, the usual procedure based on some kinetic property, such as the Hammett  $\sigma$  constants derived from the relative reactivities  $\log k/k_0$ , is subject to changes in  $r_{DA}$  described in the foregoing section, and it is not an adequate criterion. Instead, we employ a more direct measure of the HOMO energy based on the ionization potential of a substituted benzene relative to benzene, as the indicator of electron release or electron withdrawal for substituents X and Y, respectively.<sup>79</sup> We thus define the intrinsic electronic property of a substituent as electron releasing or electron withdrawing on the basis of the HOMO energy rather than the reactivity.

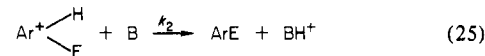
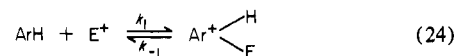
On the basis of this analysis, the para/meta isomer distribution would be simply predicted from the ionization potential of the monosubstituted benzene, as derived in the Experimental Section and summarized in Chart I. Such a prediction is nicely borne out in Figure 8, in which the para and meta isomers obtained from the variety of electrophilic aromatic substitutions included in Table V are plotted against the ionization potential of the monosubstituted benzene.<sup>80,81</sup> Four features included in Figure 8 are noteworthy. First, the monosubstituted benzenes fall rather cleanly into one of two categories, i.e., heavily para or heavily meta producing, with no arene yielding competitive amounts of each isomer.<sup>82-84</sup> Second, the isomer distributions are determined solely

by the ionization potential of the arene and are more or less independent of the electrophile. Third, the halogen substituents, F, Cl, Br, and I are clearly to be included among the electron-releasing X, and no ad hoc explanation is required to account for the isomer distributions derived from the halobenzenes. Fourth and most importantly, there is an interesting discontinuous transition from para-producing aromatics to meta-producing aromatics, and vice versa, which occurs at benzene ( $I_D = 9.23$  eV). All of these phenomena are in exact accord with the predictions in Scheme I and Chart I. Although the first three have been previously rationalized, the fourth phenomenon is not easily accounted for on the basis of conventional arguments. According to Scheme I, the discontinuity of the isomer distribution at the benzene interface is caused by the splitting of the degenerate  $e_{1g}$  orbitals by the introduction of a substituent. It is noteworthy that such a splitting can arise from even minor perturbations, such as the mere replacement of hydrogen by deuterium. This extreme sensitivity is forcefully brought forth by the remarkable inequivalency of the proton splittings in the monodeuteriobenzene ion radical below.<sup>85</sup>



Such an observed departure of the odd-electron spin density from that of the benzene ion can only arise by lifting the degeneracy of the A and S orbitals by the placement of a neutron.

**IV. The CT Formulation and the Kinetic Isotope Effects in Electrophilic Aromatic Substitutions.** Studies of the kinetic hydrogen isotope effect have played an important role in the description of electrophilic aromatic substitutions in terms of the general mechanism shown in eq 24 and 25.<sup>86</sup> According to this



formulation, the absence of hydrogen isotope effects results from proton loss in eq 25 which is faster than reversion of the intermediate in eq 24, i.e.,  $k_{-1}/k_2[\text{B}] \ll 1$ . Such a kinetic situation is tantamount to the rate-limiting formation of the intermediate in eq 24, and it is commonly encountered in nitrations and halogenations.<sup>87</sup> The CT formulation of the transition state for electrophilic aromatic substitution is also best fitted to describe this kinetic situation.<sup>88,89</sup> The other kinetic extreme in which the proton loss in eq 25 is rate limiting (i.e.,  $k_{-1}/k_2[\text{B}] \gg 1$ ) can result in sizeable kinetic isotope effects.<sup>90</sup> In this regard it is noteworthy that kinetic isotope effects have been reported for the mercuration of benzene in which  $k_{\text{H}}/k_{\text{D}} = 6.75$  at 40 °C with mercuric perchlorate in aqueous perchloric acid<sup>91</sup> and  $k_{\text{H}}/k_{\text{D}} = 6.0$  at 25 °C with mercuric acetate in aqueous acetic acid con-

(79) Since we are primarily concerned with relative effects, most ambiguities relating to the applicability of Koopman's theorem are cancelled out.

(80) (a) Turner, D. W.; Baker, C.; Baker, A. D.; Brundle, C. R. "Molecular Photoelectron Spectroscopy"; Wiley-Interscience: London, 1970. (b) Bock, H.; Wagner, G.; Kroner, J. *Tetrahedron Lett.* **1971**, *40*, 3713; *Chem. Ber.* **1972**, *105*, 3850. (c) Maier, J. P.; Turner, D. W. *Discuss. Faraday Soc.* **1972**, *54*, 149. (d) Pignataro, S.; Modelli, A.; DiStefano, G. *Justus Liebigs Ann. Chem.* **1974**, *64*, 139. (e) Foffani, A.; Pignataro, S.; Cantone, B.; Grasso, F. Z. *Phys. Chem. (Wiesbaden)* **1964**, *42*, 221. The value for PhCO<sub>2</sub>Me was taken to be the same as that for PhCO<sub>2</sub>Et. (f) Rabalais, J. W.; Colton, R. J. *J. Electron. Spectrosc. Relat. Phenom.* **1972**, *73*, 1, 83.

(81) (a) The values of the ionization potentials are chosen from the relatively recent data obtained with photoelectron spectroscopy (PES) in ref 33 and 80. The values reported by the different research groups generally agree to within 0.05 eV. For the other literature, see the references cited in ref 16 and those below. (b) Clark, D. T.; Kilcast, D.; Adams, D. B.; Scanlan, I. J. *Electron. Spectrosc. Relat. Phenom.* **1972**, *73*, 1, 153. (c) Bernardi, F.; DiStefano, G.; Mangini, A.; Pignataro, S.; Spunta, G. *Ibid.* **1975**, *7*, 457. (d) Debies, I. P.; Rabalais, J. W. *Ibid.* **1972**, *73*, 1, 355. (e) Maier, J. P.; Turner, D. W. *J. Chem. Soc., Faraday Trans. 2* **1973**, 521. (f) Neijzen, B. J. M.; de Lange, C. A. J. *Electron. Spectrosc. Relat. Phenom.* **1978**, *14*, 187. (g) Griebel, R.; Hohlneicher, G.; Dörr, F. *Ibid.* **1974**, *4*, 185. (h) Turner, D. W. *Adv. Phys. Org. Chem.* **1966**, *4*, 31. (i) Meeks, J.; Wahlborg, A.; McGlynn, S. P. *J. Electron. Spectrosc. Relat. Phenom.* **1981**, *22*, 43.

(82) (a) Brown's selectivity relationship<sup>18</sup> is based on the para/meta isomer ratio. (b) Ortho substitution has been omitted, since it is known to be strongly influenced by steric and field effects,<sup>73</sup> as well as complexation,<sup>83</sup> which are not easily evaluated. (c) Owing to field effects, we have not included benzylic and charged substituents such as -CH<sub>2</sub>NMe<sub>3</sub><sup>+</sup>, -SMe<sub>2</sub><sup>+</sup>, etc. See ref 73. (d) A further analysis of substituents and electrophiles which afford comparable amounts of meta and para products would provide an interesting test. See: Noller, C. R. "Chemistry of Organic Compounds", 3rd ed.; W. B. Saunders: Philadelphia, 1965; p 475 ff and ref 73 for some possibilities.

(83) McKillop, A.; Hunt, J. D.; Zelesko, M. J.; Fowler, J. S.; Taylor, E. C.; McGillivray, G.; Kienzle, F. J. *Am. Chem. Soc.* **1971**, *93*, 4841, 4845 and related papers.

(84) There are uncertainties in the reported isomer distributions. For example, the possibility of nonkinetic control has been raised in some electrophilic aromatic substitutions. See ref 20a, 83, and Brown, H. C.; Goldman, G. *J. Am. Chem. Soc.* **1962**, *84*, 1650. Brown, H. C.; Dubeck, M. *Ibid.* **1959**, *81*, 5608. See also: Cacace, F.; Ciranni, G.; Giacomello, P. *Ibid.* **1981**, *103*, 1513.

(85) (a) Wertz, J. E.; Bolton, J. R. "Electron Spin Resonance"; McGraw-Hill: New York, 1972; p 101-102. (b) It must be emphasized that the predictions in Chart I are qualitative, since it is known that the counterion can influence the spin densities in ion radicals. (See, for example: Sharp, J. H.; Symons, M. C. R. In "Ions and Ion Pairs in Organic Reactions"; Szwarc, M., Ed.; Wiley-Interscience: New York, 1972; Vol. 1, Chapter 5.

(86) Melander, L.; Saunders, W. H., Jr. "Reaction Rates of Isotopic Molecules"; Wiley: New York, 1980; p 162 ff.

(87) Zollinger, H. *Adv. Phys. Org. Chem.* **1964**, *2*, 163.

(88) Under these circumstances, only a secondary kinetic isotope effect is predicted by the CT formulation (see: Klingler, R. J.; Mochida, K.; Kochi, J. K. *J. Am. Chem. Soc.* **1979**, *101*, 6626).

(89) The secondary kinetic isotope for the mercuration of toluene- $\alpha,\alpha,\alpha$ -d<sub>3</sub> by mercuric acetate in aqueous acetic acid containing perchloric acid is reported to be  $1.00 \pm 0.03$  per deuterium (Swain, C. G.; Knee, T. E. C.; Kresge, A. J. *J. Am. Chem. Soc.* **1957**, *79*, 505).

(90) Taylor, R. *Compr. Chem. Kinet.* **1972**, *13*, 1.

(91) Perrin, C.; Westheimer, F. H. *J. Am. Chem. Soc.* **1963**, *85*, 2773.

taining perchloric acid.<sup>92</sup> Let us assume for the moment that similar values of the hydrogen isotope effect obtain with mercuric trifluoroacetate in the nonaqueous solvents examined in this study. If so, the inclusion of mercuration in Figure 5 and in eq 10 suggests that the CT formulation is not necessarily restricted to aromatic substitutions in which the formation of the intermediate is rate limiting. However, the extent to which the CT formulation will generally describe the activation process for aromatic substitutions in which proton loss is rate limiting remains to be determined in further studies.<sup>93</sup>

### Summary and Conclusion

The disappearance of the transient charge-transfer (CT) absorption bands  $h\nu_{CT}$  coincides with the electrophilic aromatic substitution with bromine, chlorine, and mercury(II) electrophiles. The relative reactivity  $\log k/k_0$  of various arenes to halogenation and mercuration in Figure 6 is equal to the relative CT transition energies  $\Delta h\nu_{CT}$ , using benzene as the reference (eq 10). From Mulliken theory, the CT transition represents a vertical excitation to the ion-pair state  $[Ar^+E^-]^*$ , which accords with direct observations by pulsed laser spectroscopy.<sup>41</sup> Thus the activated complex for electrophilic aromatic substitution can also be described as an ion pair. For the CT excited ion pair in eq 11 to be equated to the ion pair derived by the thermal, adiabatic process in eq 12, the solvation energies of the series of aromatic cations must be constant. Indeed, independent electrochemical measurements have established the direct relationship between the cyclic voltammetric peak potentials  $E_p$  for anodic oxidation with the gas-phase ionization potentials  $I_D$ —showing the constancy of the solvation terms  $\Delta G^s$  for these aromatic cations.

The charge-transfer formulation in eq 10 relates directly to other linear free energy relationships which have been previously established for electrophilic aromatic substitution. For example, the  $\rho$  value in the correlation with the  $\sigma^+$  substituent constants is proportional to  $\alpha_E$  in eq 19. The magnitude of  $\alpha_E$  represents the slope of the relationship between  $\Delta h\nu_{CT}$  and  $\Delta I_D$  and, as such, reflects the changes in  $r_{DA}$  for aromatic substitution (eq 22). Other linear free energy relationships such as those involving the proton affinity or the  $\sigma$  basicity of arenes are similarly accommodated within the CT framework.

The charge-transfer formulation also provides unique insight into the origin of the isomeric product distribution. Following the rate-limiting formation of the ion pair, the regioselectivity in its collapse in eq 23 is determined by the odd-electron distribution in the aromatic cation. This is supported by the strong correlation which is observed between the isomeric product distribution and the spin densities, independently determined from the ESR parameters of the aromatic ion radicals. Furthermore it predicts in Scheme I, the change in meta/para isomer ratios from monosubstituted benzenes when electron-withdrawing substituents are replaced with electron-releasing substituents (Figure 8). The directive properties of the halogen substituents, which have hitherto been subjected to ad hoc explanations, evolve naturally from the CT formulation.

### Experimental Section

**Materials.** Benzene, the monosubstituted benzenes, and the disubstituted benzenes (Aldrich Chemical Co.) were purified by repeatedly shaking them with successive portions of cold concentrated  $H_2SO_4$ , until the lower layer was colorless. The aromatic layer was washed with aqueous  $NaHCO_3$ , followed by several washings with water, and dried over  $CaCl_2$ . The arene was then distilled from sodium. This procedure could not be applied to mesitylene since the sulfonation of mesitylene occurred too readily. Thus mesitylene was initially sulfonated by dissolving it in concentrated  $H_2SO_4$ . Mesitylenesulfonic acid was precipitated by the addition of concentrated  $HCl$  at 0 °C, washed with cold

concentrated  $HCl$ , and recrystallized from  $CHCl_3$ . The sulfonic acid was hydrolyzed by boiling it in 20% aqueous  $HCl$ , and the separated mesitylene was dried over  $CaCl_2$  and distilled from sodium. Tetramethylbenzene, hexamethylbenzene, hexaethylbenzene, and *p*-dimethoxybenzene were purified by recrystallization from absolute ethanol. Mercury trifluoroacetate, bromine and chlorine used in this study were described previously.<sup>16</sup> Methylene chloride used as a solvent was reagent grade material obtained commercially and purified according to a standard method.<sup>94</sup> Since the presence of water in trifluoroacetic acid is known to cause an acceleration of the bromination rate for toluene,<sup>26</sup> it was purified according to the standard method to remove water.<sup>29,95</sup> Accordingly, trifluoroacetic acid obtained commercially was refluxed with phosphorous pentoxide for several hours and then was fractionally distilled through a 20-plate Oldershaw column. Trifluoroacetic anhydride (~2% v) was added, and the resulting anhydrous trifluoroacetic acid was stored under argon. Reagent grade acetonitrile was stirred with calcium hydride overnight. After filtration, the acetonitrile was treated with potassium permanganate and redistilled from phosphorous pentoxide under a nitrogen atmosphere.

**Spectral Measurements of the CT Absorption Bands.** The charge-transfer spectra in Figure 1 and the transition energies in Tables I and II were described previously.<sup>16</sup> All the CT parameters were obtained by measuring the difference spectra under carefully calibrated conditions in order to exclude the overlapping bands arising from the arenes and the electrophiles.

**Kinetic Measurements. Mercuration.** The rate of the mercuration of arenes with  $Hg(O_2CCF_3)_2$  in methylene chloride was followed spectroscopically on a Cary 14 spectrophotometer by the disappearance of  $Hg(O_2CCF_3)_2$ , as well as by the decay of the CT absorbance. A stock solution of  $5.0 \times 10^{-3}$  to  $2.0 \times 10^{-2}$  M  $Hg(O_2CCF_3)_2$  was freshly prepared immediately prior to the kinetic run. The reaction was carried out in a 10-mm quartz cuvette placed in the thermostated compartment of the spectrophotometer and maintained at  $25.0 \pm 0.3$  °C. The reaction was initiated by injecting a known amount of arene into the cuvette with the aid of a glass microsyringe. The addition was accompanied by a vigorous shaking of the cuvette. Aliquots of the reaction mixture (20  $\mu L$ ) were withdrawn periodically and quickly added to another 10-mm quartz cuvette containing  $2.5 \times 10^{-3}$  M potassium iodide in aqueous methanol. The latter was of such a composition that the final solution had a mole fraction of 0.91 for MeOH. By this procedure,  $Hg(O_2CCF_3)_2$  was quantitatively converted to triiodomercurate(II) instantaneously. Following this, the concentration of the  $Hg(II)$  derivatives during the reaction was determined from the absorbance of  $HgI_3^-$  at 301.5 nm by using the calibrated equation developed by Abraham and Johnston.<sup>21</sup> This quenching method was used to follow the kinetics of the slow reactions. The rate expression in eq 6 was confirmed by using the second-order relationship presented in eq 26 for equimolar amounts of each

$$1/C = 2kt + 1/C_0 \quad (26)$$

reactant, as shown in Figure 2a, where  $C$  and  $C_0$  are the concentration of the reactant at time  $t$  and its initial concentration, respectively. With excess arene, the second-order kinetics in eq 6 lead to the pseudo-first-order plots shown in Figure 2b.

The decay of the CT absorbance was also followed spectrophotometrically at the wavelengths where the absorbance results principally from the CT bands (>95%) with negligible overlap with the absorbance due to the reactants. The wavelengths chosen to follow the decay of the CT absorbance were 355 nm for mesitylene, 320 nm for anisole, 310 nm for substituted dimethylbenzenes, and 290 nm for the other arenes. The kinetics of the decay of the CT absorbance  $\mathcal{A}$  followed eq 27. The rate

$$-d\mathcal{A}/dt = k\{[Ar] + [Hg(O_2CCF_3)_2]\}\mathcal{A} \quad (27)$$

constants expressed in units of  $M^{-1} s^{-1}$  for eq 27 were determined by the pseudo-first-order plots in Figure 2b, in the presence of excess arene. The rate constants determined by eq 27 agreed with those obtained from the disappearance of  $Hg(O_2CCF_3)_2$ , to within experimental error. For example, the rate constant for cumene was determined to be  $1.4 \times 10^{-3} M^{-1} s^{-1}$  by eq 6 from the plot in Figure 2b. The same value,  $1.4 \times 10^{-3} M s^{-1}$ , was obtained by the use of eq 27. For mesitylene, the second-order plot in Figure 2a gave  $k = 0.33 M^{-1} s^{-1}$  from eq 26; and the pseudo-first-order plot of the CT absorbance in Figure 2b gave  $k = 0.41 M^{-1} s^{-1}$  by eq 27. The rate constants for the other compounds determined by both methods (eq 6 and eq 27) agreed to within 20%. In fact, eq 27 can

(92) Kresge, A. J.; Brennan, J. F. *Proc. Chem. Soc., London* 1963, 215; *J. Org. Chem.* 1967, 32, 752.

(93) The extent to which the CT formulation applies to aromatic substitutions involving rate-limiting proton loss will probably depend on the similarity of this transition state with the intermediate. For a discussion of Hammond's postulate as it applies to electrophilic aromatic substitution, see: Carey, F. A.; Sundberg, R. J. "Advanced Organic Chemistry", Part A; Plenum Press: New York, 1977; p 398 ff.

(94) Perrin, D. D.; Armarego, W. L. F.; Perrin, D. R. "Purification of Laboratory Chemicals"; Pergamon Press: Elmsford, NY, 1968.

(95) (a) The dielectric constant of trifluoroacetic acid with the absence of water,  $\epsilon_B = 8.5^{79b}$  is significantly smaller than that of unpurified trifluoroacetic acid,  $\epsilon_B = 42.1$  at 25 °C.<sup>88c</sup> (b) Harris, F. E.; O'Konski, C. T. *J. Am. Chem. Soc.* 1954, 76, 4317. (c) Simons, J. H.; Lorentzen, K. E. *Ibid.* 1950, 72, 1426.

be derived from eq 6. Thus the differentiation of eq 4 with respect to time, yields

$$\frac{-d\mathcal{A}}{dt} = \epsilon K \left\{ [\text{Ar}] \frac{d[\text{Hg}(\text{O}_2\text{CCF}_3)_2]}{dt} + [\text{Hg}(\text{O}_2\text{CCF}_3)_2] \frac{d[\text{Ar}]}{dt} \right\} \quad (28)$$

With use of the relationship,  $d[\text{Hg}(\text{O}_2\text{CCF}_3)_2]/dt = d[\text{Ar}]/dt$  together with eq 4, eq 28 will be reexpressed as eq 27.

**Bromination.** The rate of the bromination of arenes in trifluoroacetic acid was followed by the disappearance of the bromine absorbance at  $\lambda_{\text{max}}$  411 nm ( $\epsilon_{\text{max}}$  138),<sup>29</sup> as well as by the decay of the CT absorbance. A stock solution of bromine in  $\text{CF}_3\text{CO}_2\text{H}$  ( $5.43 \times 10^{-3}$ – $8.93 \times 10^{-2}$  M) was freshly prepared from purified bromine which was vacuum transferred from  $\text{P}_2\text{O}_5$  and kept under argon. The kinetic study was carried out at 25 °C in a Schlenk tube equipped with a small side arm fused onto a square quartz cuvette (i.d. = 10 mm). Adventitious room light was carefully excluded from the bromination reaction to avoid the radical chain substitution by bromine atom.<sup>26</sup> Moreover, it was confirmed that the observed rate was unaffected by the monitoring light, by periodically shuttering the spectrophotometer. It was also shown that there was no interference from species such as  $\text{Br}_3^-$ , since the change of the ratio of the absorbance during the reaction relative to the initial value, i.e.,  $(\mathcal{A} - \mathcal{A}_\infty)/\mathcal{A}_0$ , was independent of the wavelength used to monitor the reaction in the presence of excess arene.

The same second-order kinetics as those obtained in mercuriation was applied to the bromination. The pseudo-first-order rate constants,  $k_p$ , obtained in the presence of excess arene showed the same linear dependence on the concentrations of arene, as illustrated in Figure 3. For each arene, the ratio of the  $\text{Br}_2$  concentration during the reaction to the initial value, i.e.,  $[\text{Br}_2]/[\text{Br}_2]_0$  was the same as the ratio of the CT absorbances,  $\mathcal{A}/\mathcal{A}_0$ , in the presence of excess of aromatics. The CT absorbance was followed at wavelengths between 300 nm and approximately 330 nm, where the absorbance due to  $\text{Br}_2$  was negligible compared to the CT absorbance (<5%). The rate constants obtained from both methods agreed to within experimental error with those determined by the titrimetric method, for some of the compounds listed in Table II (see the footnote a).<sup>20b</sup>

**Cyclic Voltammetry of Arenes.** Single-sweep cyclic voltammograms (CV) of the aromatic compounds ( $\sim 1.0 \times 10^{-2}$  M) listed in Table III were carried out with a stationary platinum microelectrode at 25 °C in acetonitrile and trifluoroacetic acid solutions. The supporting electrolytes used were 0.1 M sodium perchlorate and tetraethylammonium perchlorate for acetonitrile and trifluoroacetic acid solutions, respectively. The electrochemical instrumentation used in this study was described elsewhere.<sup>31</sup> The platinum electrode was routinely cleaned for each measurement by soaking it in concentrated nitric acid for 1 h. It was then rinsed repeatedly with distilled water and dried at 120 °C for 2 h prior to use. At the sweep rate of 100  $\text{mV s}^{-1}$ , all the compounds listed in Table III showed distinctive current maxima of the anodic waves, in accord with electrochemical theory.<sup>31,34</sup> No cathodic waves on the reverse scan were observed at various sweep rates in the range between 100 and 900  $\text{mV s}^{-1}$ , except for hexaethylbenzene and *p*-dimethoxybenzene. The widths of the anodic waves ( $E_p - E_{p/2}$ ) varied between 0.1 and approximately 0.4 V at a sweep rate of 100  $\text{mV s}^{-1}$ , depending upon the arene and the solvent. With an increase in the sweep rate, the peaks of the anodic waves broadened somewhat and yielded a current plateau for the less reactive compounds such as benzene. This broadening may be caused by absorption effects, since benzene is known to have a weak interaction with platinum electrodes, particularly at anodic potentials.<sup>36</sup> Thus, the

(96) (a) Sathyanarayana, S. *J. Electroanal. Chem.* **1965**, *10*, 119. (b) Lipkowski, J.; Galus, Z. *Ibid.* **1975**, *61*, 11. (c) Dutkiewicz, E.; Puacz, A. *Ibid.* **1979**, *100*, 947. (d) Gileadi, E.; Duic, L.; Bockris, J. O'M. *Electrochim. Acta* **1968**, *13*, 1915.

(97) (a) Komatsu, T.; Lund, A.; Kinell, P. O. *J. Phys. Chem.* **1972**, *76*, 1721. (b) Dixon, W. T.; Murphy, D. *J. Chem. Soc., Perkin Trans. 2* **1976**, 1823. (c) Dixon, W. T.; Murphy, D. *J. Chem. Soc., Faraday Trans. 2* **1976**, *72*, 1221. (d) Bolton, J. R.; Carrington, A. *Mol. Phys.* **1961**, *4*, 497. (e) Bowers, K. W. In "Radical Ions"; Kaiser, E. T., Kevan, L., Eds.; Wiley-Interscience: New York, 1968; Chapter 5. (f) Rudenko, A. P.; Zarubin, M. Ya.; Aveyanov, S. F.; Barsheva, N. S. *Dokl. Akad. Nauk SSSR* **1979**, *249*, 117. (These are 3,5-dimethyl-substituted compounds. Since the spin distributions are perturbed by the methyl substitution, the assignment of these cations to type A is obviously based on the small hfs on the para positions.) (g) Rieger, P. H.; Bernal, I.; Reinmuth, W. H.; Fraenkel, G. K. *J. Am. Chem. Soc.* **1963**, *85*, 683. (h) Rieger, P. H.; Fraenkel, G. K. *J. Chem. Phys.* **1963**, *39*, 609. (i) Wilson, R. *Can. J. Chem.* **1966**, *44*, 551.

Table VI. Proton Hyperfine Coupling Constants in Monosubstituted Benzene Ion Radicals

aromatic ion radical		$a_H$ for ring protons, G			ref <sup>a</sup>
substituent	charge	o	m	p	
$\text{CH}_3$	cation	2.1	0	11.8	<i>a</i>
$\text{CH}_3\text{O}$	cation	5.0	0.5	10.6	<i>b</i>
HO	cation	5.3	0.8	10.7	<i>c</i>
NC	cation	9.15	11.45	0	<i>f</i>
$\text{HO}_2\text{C}$	cation	9.05	11.85	0.75	<i>f</i>
$\text{CH}_3$	anion	5.12	5.45	0.59	<i>d</i>
$\text{CH}_3\text{O}$	anion	5.34	6.06	0.64	<i>e</i>
NC	anion	3.63	0.30	8.42	<i>g</i>
$\text{O}_2\text{N}$	anion	3.36	1.07	4.03	<i>h</i>
OHC	anion	4.26	1.36	6.24	<i>i</i>
		5.14	1.62		

<sup>a</sup> Cited in ref 97.

values of the anodic peak potentials in Table III (the potentials relative to saturated NaCl SCE were always taken from the measurement of the first scan at the sweep rate of 100  $\text{mV s}^{-1}$ , where the shape of the anodic CV waves were optimized. The values of the peak potentials for the first scan were reproducible to within  $\pm 50$  mV for different runs, when the standard cleaning procedure of the electrode mentioned above was applied. For each run in acetonitrile, a small amount of ferrocene was added as an internal standard. Repeated CV scans affected the positions of the peak potentials of the arene slightly, accompanied by a similar shift ( $\sim 50$  mV increase after 10 scans) of the standard. Thus, the apparent deterioration of the electrode by repeated scans can be corrected by calibrating on the potential shift of the standard.

**Odd-Electron Spin Densities in Aromatic Ion Radicals.** For aromatic ion radicals, the unpaired  $\pi$ -electron density on carbon  $\rho_C$  is proportional to the ESR hyperfine coupling constant  $a_H$  of the proton attached to the carbon center, i.e.<sup>85</sup>

$$a_H = Q\rho_C$$

The assignment of the HOMO orbitals as S or A in Scheme I can thus be carried out by attributing the largest value of  $a_H$  at the para position to S and the smallest  $a_H$  at the para position as belonging to A. Accordingly, from the experimental values of  $a_H$  listed in the top half of Table VI for the monosubstituted benzene cation radicals the HOMO assignment for the electron-releasing substituents X =  $\text{CH}_3$ ,  $\text{OCH}_3$ , and OH is confirmed as S and for the electron-withdrawing substituents Y = CN and  $\text{CO}_2\text{H}$  it is A.<sup>98</sup>

The availability of the ESR spectra of aromatic anion radicals provides a further confirmation of this orbital assignment. Since the HOMO in the benzene anion radical is the antibonding  $e_{2u}$  the orbital assignment in the monosubstituted anion radical for S and A should be reversed relative to that in the corresponding cation radical.<sup>78</sup> Indeed, the relative values of  $a_H$  listed in the bottom half of Table VI for the meta and para positions of anion radicals are reversed relative to those of cation radicals.

Although the spin densities in the 2- and 3-positions are the same in the benzene cation radical, upon the introduction of substituent X or Y they are no longer the same, as indicated by the ESR data in Table VI. For Ph-X, the spin density at the ortho position is larger than that at the meta position, and in Ph-Y the opposite pertains. The predictions of the relative isomer distributions in Chart I is based on these spin densities. Furthermore in Ph-Y, the spin density in the ortho position is larger than that in the para position. Thus ortho substitution should track meta substitution better than para substitution, in the absence of field and related ortho effects.

**Acknowledgment.** We wish to thank the National Science Foundation for financial support of this research, K. S. Chen for the measurement of the CT spectrum of the nitronium-arene complex in Figure 1d, and the Halocarbon Products Corp. for a generous gift of trifluoroacetic acid.

(98) It should be noted, however, that the HOMO of cyanobenzene was assigned as  $e_{1g}(\text{S})$  in the photoelectron spectrum.<sup>33c</sup> However, the theoretical assignment is A like that in Table VI. (Bernardi, F.; Guerra, M.; Pedullì, G. *F. Tetrahedron* **1978**, *34*, 2141.)